GRAPHENE BASED OPTICAL MODULATOR USING FINITE DIFFERENCE TIME DOMAIN METHOD

By

Adan Saeed

(Registration No: 00000330413)

Department of Electrical Engineering and Computer Science (SEECS)

National University of Sciences and Technology (NUST)

Islamabad, Pakistan

(2024)

GRAPHENE BASED OPTICAL MODULATOR USING FINITE DIFFERENCE TIME DOMAIN METHOD

By Student Name: **Adan Saeed**

(Registration No: 00000330413)

A thesis submitted to the National University of Sciences and Technology, Islamabad,in partial fulfillment of the requirements for the degree of

Masters of Telecommunication

Supervisor: **Dr. Mohaira Ahmad**

School of Electrical Engineering and Computer Science (SEECS)

National University of Sciences and Technology (NUST)

Islamabad, Pakistan

(2024)

THESIS ACCEPTANCE CERTIFICATE

Certified that final copy of MS/MPhil thesis entitled "Graphene based optical modulator using finite difference time domain method" written by Adan Saeed, (Registration No 00000330413), of SEECS has been vetted by the undersigned, found complete in all respects as per NUST Statutes/Regulations, is free of plagiarism, errors and mistakes and is accepted as partial fulfillment for award of MS/M Phil degree. It is further certified that necessary amendments as pointed out by GEC members of the scholar have also been incorporated in the said thesis.

Signature: _____   ____   ____

Name of Advisor: ____Dr. Mohaira Ahmad____ __

Date: _____27-May-2024____ __

HoD/Associate Dean:_____

Date: _____27-May-2024_____

Signature (Dean/Principal): _____ __

Date: _____27-May-2024_____ __

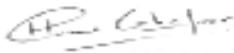# National University of Sciences & Technology
MASTER THESIS WORK

We hereby recommend that the dissertation prepared under our supervision by: (Student Name & Reg. #) Adan Saeed [00000330413]

Titled: Graphene based optical modulator using finite difference time domain method

be accepted in partial fulfillment of the requirements for the award of Master of Science (Electrical Engineering) degree.

Examination Committee Members

1. Name: Salman Abdul Ghafoor   Signature: _____
   22-Jul-2024 10:32 PM

2. Name: Huma Ghafoor   Signature: _____
   22-Jul-2024 10:32 PM

Supervisor's name: Mohaira Ahmad   Signature: _____
24-Jul-2024 10:55 AM

_____
Salman Abdul Ghafoor
HoD / Associate Dean

23-July-2024
Date

COUNTERSINGED

25-July-2024
Date

_____
Muhammad Ajmal Khan
Principal

CERTIFICATE OF APPROVAL

Approval

It is certified that the contents and form of the thesis entitled "Graphene based optical modulator using finite difference time domain method" submitted by Adan Saeed have been found satisfactory for the requirement of the degree

Advisor :   Dr. Mohaira Ahmad

Signature: _____

Date: _____27-May-2024_____

Committee Member 1:Dr. Salman Abdul Ghafoor

Signature: _____

26-May-2024

Committee Member 2:Dr. Huma Ghafoor

Signature: _____

Date: _____24-May-2024_____

AUTHOR'S DECLARATION

I Adan Saeed hereby state that my MS thesis titled "GRAPHENE BASED OPTICAL MODULATOR USING FINITE DIFFERENCE TIME DOMAIN METHOD" is my own work and has not been submitted previously by me for taking any degree from National University of Sciencesand Technology, Islamabad or anywhere else in the country/ world. At any time if my statement is found to be incorrect even after I graduate, the universityhas the right to withdraw my MS degree.

Student Signature: Adan Saeed

Name: Adan Saeed

Date: 7/25/2024

PLAGIARISM UNDERTAKING

I solemnly declare that research work presented in the thesis titled "GRAPHENE BASED OPTICAL MODULATOR USING FINITE DIFFERENCE TIME DOMAIN METHOD" is solely my re- search work with no significant contribution from any other person. Small contribution/help wherever taken has been duly acknowledged and that complete thesis has been written by me.

I understand the zero-tolerance policy of the HEC and National University of Sciences and Technology (NUST), Islamabad towards plagiarism. Therefore, I as an author of the above titled thesis declare that no portion of my thesis has been plagiarized andany material used as reference is properly referred/cited.

I undertake that if I am found guilty of any formal plagiarism in the above titled thesis even after award of MS degree, the University reserves the rights to withdraw/revoke my MS degree and that HEC and NUST, Islamabad has the right to publish my name on the HEC/University website on which names of students are placed who submitted plagiarized thesis.

Student Signature: Adan Saeed

Name: Adan Saeed

DEDICATED

TO

MY FAMIY

ACKNOWLEDGEMENTS

ABSTRACT

The thesis titled " GRAPHENE BASED OPTICAL MODULATOR USING FINITE DIFFERENCE TIME DOMAIN METHOD" investigates the performance and potential of graphene-based optical modulators in advancing optical communication systems. Utilizing the Finite-Difference Time-Domain (FDTD) method, this research models the interaction between light and graphene within an optical waveguide, focusing on key parameters such as applied voltage, electric field strength, and carrier mobility. The findings reveal that graphene-based modulators exhibit high modulation efficiency across a broad range of frequencies, from visible to terahertz, due to graphene's unique properties, including high carrier mobility and ultra-fast response times.

The study demonstrates that optimal modulation efficiency is achieved at specific bias voltages and field strengths, underscoring the importance of precise parameter control. Additionally, the seamless integration of graphene with existing silicon photonics technologies enhances the functionality of current photonic devices without requiring substantial manufacturing changes. The research emphasizes graphene's suitability for low-power, high-speed optical modulation, applicable in high-speed data transmission and terahertz signal processing.

A comprehensive literature review provides context by comparing traditional optical modulators and recent advancements in the field, highlighting graphene's potential to overcome the limitations of conventional materials. The methodology section details the simulation setup, including domain size, grid resolution, boundary conditions, and the initialization of field variables, offering insights into the simulation's accuracy and reliability.

Results and discussions focus on the electric and magnetic field distributions, modulation efficiency, and the effects of various parameters. Comparisons with existing work highlight the improvements in modulation efficiency and potential for integration with silicon photonic technologies. The conclusion summarizes the key findings, emphasizing the high modulation efficiency and broadband capabilities of graphene-based modulators, and suggests future research directions, including optimizing fabrication techniques and exploring environmental effects on device stability.

Overall, this thesis provides a detailed analysis of graphene-based optical modulators, demonstrating their potential to revolutionize optical communication systems with high-speed, energy-efficient, and versatile solutions.

Keywords: Graphene Optical Modulator, Finite-Difference Time-Domain (FDTD), Modulation Efficiency, Silicon Photonics, High-Speed Data Transmission

TABLE OF CONTENTS

LIST OF FIGURES

LIST OF TABLES

LIST OF ABBREVIATIONS

Abbreviation	Definition
2D	Two-Dimensional
BBG	Bragg Grating
c	Speed of Light
CFL	Courant-Friedrichs-Lewy
DC	Direct Current
EAM	Electro-Absorption Modulator
ER	Electro-Refraction
FDTD	Finite-Difference Time-Domain
FET	Field-Effect Transistor
GHz	Gigahertz
HMM	Hyperbolic Metamaterials
J	Electric Current Density
m	Meter
MZI	Mach-Zehnder Interferometer
MWP	Microwave Photonic
nm	Nanometer
PML	Perfectly Matched Layer
S	Siemens
SPP	Surface Plasmon Polariton
THz	Terahertz
TIR	Total Internal Reflection
PML	Perfectly Matched Layer
W/mK	Watts per Meter-Kelvin

CHAPTER: 1   INTRODUCTION

1.1   Background

Optical modulators are crucial components in modern optical communication systems, enabling the manipulation of light signals to encode information. These devices modulate the intensity, phase, or polarization of light, allowing for high-speed and low-loss data transmission over optical fibers. Traditional modulators, such as electro-optic modulators based on lithium niobate (LiNbO3), are widely used due to their fast response times and high efficiency (Yariv & Yeh, 2007). Graphene, a two-dimensional material consisting of a single layer of carbon atoms arranged in a hexagonal lattice, has attracted significant attention in photonics due to its exceptional optical and electronic properties, including high carrier mobility, broadband optical absorption, and tunable electronic properties, making it ideal for optical modulation applications (Bonaccorso et al., 2010). Unlike traditional materials, graphene can achieve modulation over a broad range of wavelengths, from visible to terahertz, due to its unique band structure (Bao & Loh, 2012). Graphene-based optical modulators offer advantages such as ultra-fast response times, low power consumption, and compatibility with silicon photonics, enabling dynamic control of light essential for high-speed data communication and optical signal processing (Liu et al., 2011; Phare et al., 2015). These modulators can enhance optical networks by being integrated into photonic devices like switches, filters, and detectors, thus improving the performance of optical communication systems. Key applications include high-speed data transmission, optical signal processing, on-chip integration, and terahertz communications (Romagnoli et al., 2018; Koppens et al., 2014). The development of graphene integrated optical modulators represents a significant advancement in photonics, offering high-speed, energy-efficient, and versatile solutions for future communication technologies (Koester & Li, 2012).

1.2   Objectives

The primary objectives of this research are to investigate the performance of a graphene-based optical modulator and to analyze the modulation efficiency and its dependence on various parameters. This involves a detailed study of how the modulator's efficiency is influenced by factors such as applied voltage, electric field strength, carrier concentration, and mobility. The research aims to provide insights into optimizing the design and operation of graphene integrated

optical modulators for high-speed and efficient optical communication systems. By exploring these parameters, the study seeks to enhance the understanding of graphene's role in photonic applications and to contribute to the development of advanced optical modulation technologies.

1.3 Scope of the Study

This study encompasses a comprehensive examination of several key parameters that influence the performance of a graphene-based optical modulator. The primary parameters investigated include the applied voltage to the graphene layer and its impact on the modulation efficiency and conductivity of graphene, as well as the strength and frequency of the external electric field and how it affects the modulation depth and overall performance of the optical modulator. Additionally, the study examines the variation in the refractive index due to changes in the electric field and its effect on the propagation of the optical signal through the modulator. It also considers the position and behavior of the optical beam within the waveguide, including how the beam interacts with the graphene layers and the resulting changes in the modulated signal. By focusing on these parameters, the study aims to provide a detailed understanding of the operational characteristics and optimization strategies for graphene integrated optical modulators, thereby contributing to the advancement of optical communication technologies.

1.4 Thesis outline

This thesis delves into the performance of graphene-based optical modulators and their potential to revolutionize optical communication systems. The research is motivated by the exceptional properties of graphene, including its high carrier mobility, broadband optical absorption, and tunable electronic properties. These characteristics make graphene an ideal material for optical modulation applications, offering advantages such as ultra-fast response times, low power consumption, and compatibility with silicon photonics.

The study begins with an introduction that sets the context for optical modulators in modern communication systems. It explains the role of these devices in manipulating light signals to encode information, which is essential for high-speed, low-loss data transmission. Traditional materials and methods, like electro-optic modulators based on lithium niobate, are discussed, followed by an overview of graphene's unique benefits.

A comprehensive literature review follows, providing an in-depth look at current optical modulator technologies, the integration of graphene in photonics, and the theoretical models and simulation techniques used in the field. This review highlights the advancements and limitations of existing technologies, paving the way for the proposed graphene-based solutions.

The methodology chapter outlines the simulation approach using the Finite-Difference Time-Domain (FDTD) method. Detailed descriptions of the simulation setup, including domain size, grid resolution, boundary conditions, and the initialization of field variables, are provided. The chapter explains the dynamic calculation of graphene's conductivity and the impact of applied voltage and external electric fields on the modulator's performance.

Results and discussion present a detailed analysis of the electric and magnetic field distributions, modulation efficiency, and the effects of various parameters such as applied voltage and external electric field. The performance of the modulator is evaluated through comparisons with existing work, highlighting improvements in modulation efficiency and the potential for integration with existing silicon photonic technologies.

The conclusion summarizes the key findings, emphasizing the high modulation efficiency of graphene-based modulators across a broad range of frequencies and voltages. The study underscores the suitability of graphene for high-speed, low-power optical modulation, and its compatibility with current manufacturing processes, making it a promising candidate for future optical communication systems.

The thesis also suggests future research directions, including optimizing fabrication techniques, exploring environmental effects on device stability, and further improving simulation methods. The goal is to advance the development of reliable, high-performance graphene-based optical modulators for next-generation photonic applications.

CHAPTER: 2   LITERATURE REVIEW

2.1   Overview of Optical Modulators

Optical modulators are essential components in optical communication systems, as they allow for the control and manipulation of light signals to encode information. Traditional optical modulators, such as electro-optic modulators, acousto-optic modulators, and thermo-optic modulators, have been widely used for several decades. Electro-optic modulators, which often utilize materials like lithium niobate (LiNbO3), exploit the electro-optic effect to change the refractive index of the material in response to an applied electric field, enabling the modulation of light intensity, phase, or polarization. Acousto-optic modulators, on the other hand, use sound waves to modulate the optical signal, while thermo-optic modulators rely on temperature changes to achieve modulation (Yariv & Yeh, 2007).

Recent advancements in optical modulation technology have focused on developing materials and devices that offer improved performance in terms of speed, efficiency, and integration. One significant area of progress is the integration of optical modulators with silicon photonics, allowing for the development of compact and efficient photonic integrated circuits (PICs). Silicon-based modulators, such as those using the plasma dispersion effect or carrier injection/depletion mechanisms, have shown promise for high-speed data transmission with low power consumption. Additionally, novel materials like graphene have emerged as potential candidates for next-generation optical modulators due to their exceptional electronic and optical properties. Graphene-based modulators offer ultra-fast response times, broadband modulation capabilities, and the ability to tune optical properties dynamically (Bonaccorso et al., 2010; Phare et al., 2015). These advancements are paving the way for more efficient and versatile optical communication systems, capable of meeting the increasing demands for higher data rates and lower energy consumption.

2.2   Graphene in Photonics

Graphene, a two-dimensional material composed of a single layer of carbon atoms arranged in a hexagonal lattice, exhibits exceptional properties that make it highly suitable for optical modulation. One of the most significant properties of graphene is its high carrier mobility, which allows for ultra-fast electronic response and enables high-speed optical modulation. Additionally,

graphene has a broadband optical absorption that extends from the visible to the terahertz range, making it versatile for various photonic applications. Its tunable electronic properties, controlled by electrical gating, allow dynamic adjustment of its optical properties, providing a mechanism for efficient modulation. Furthermore, graphene's compatibility with existing silicon photonics technology facilitates its integration into current photonic devices, enhancing their functionality without requiring significant changes in manufacturing processes (Bonaccorso et al., 2010; Bao & Loh, 2012).
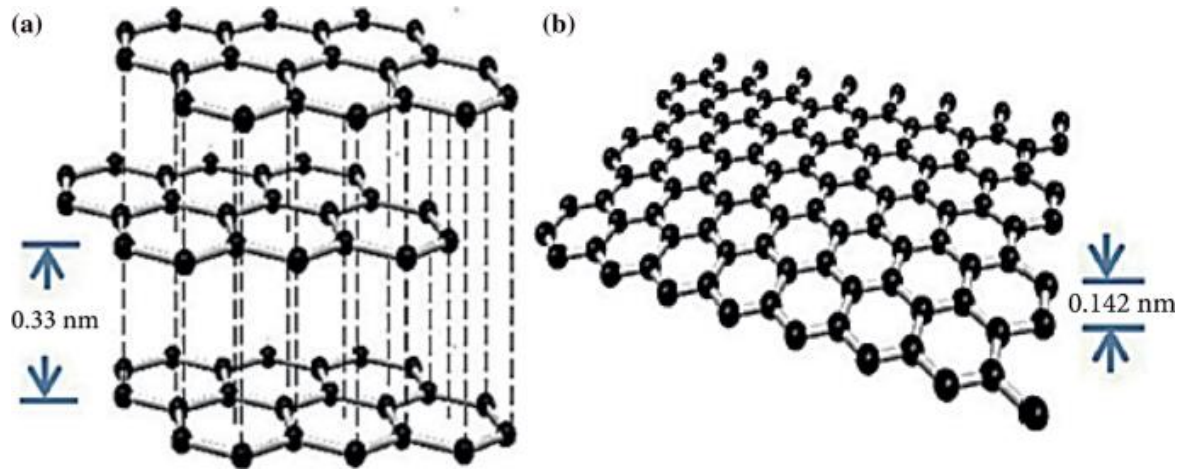
Figure 2.1: A schematic representation of graphene's hexagonal lattice structure
Source: (Ashok Kumar, Bashir, Ramesh, & Ramesh, 2022)

Graphene's unique electronic properties stem from its band structure, which can be visualized in various ways to understand its behavior under different conditions. The following figure illustrates several key aspects of graphene's electronic structure:
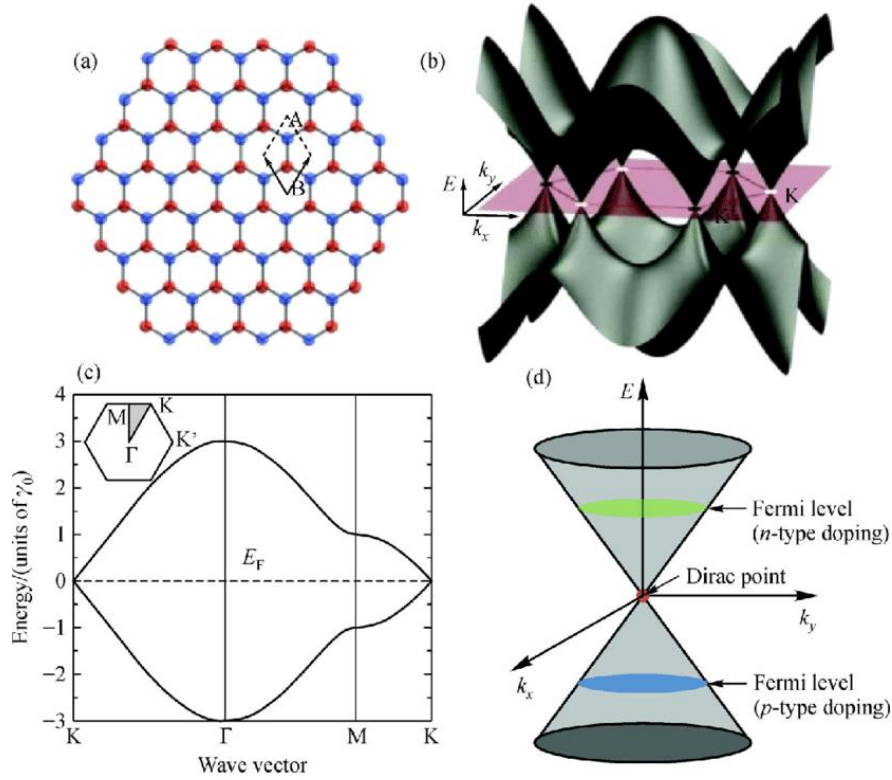
Figure 2.2: A diagram illustrating the electronic band structure of graphene, highlighting the Dirac cones.

Source: (Vasudevan, Shvalya, Zidanšek, & Cvelbar, 2019)

Graphene, due to its unique properties, has revolutionized the field of photonics and optoelectronics. The ability to tune the electronic properties of bilayer graphene has been directly observed, showcasing its potential for various photonic applications (Zhang et al., 2009). This tunability is further evidenced by the ultra-fast response times of graphene-based photodetectors, making them ideal for high-speed data communication (Xia et al., 2009). Additionally, graphene's plasmonic properties enable the creation of tunable terahertz metamaterials, enhancing functionality in this frequency range (Ju et al., 2011). The development of graphene field-effect devices has opened new avenues in electronic applications (Lemme et al., 2007), with nonvolatile switching demonstrating promising results for memory and logic devices (Echtermeyer et al., 2008). Mechanically, controlled ripple texturing can significantly influence the properties of suspended graphene, providing pathways to novel applications (Bao et al., 2009). Integrating graphene into photonic crystal slabs enhances optical absorption, which is crucial for improving device performance (Zhan et al., 2017). The creation of Van der Waals heterostructures

incorporating graphene highlights its potential for advanced device applications, further expanding its versatility (Liu et al., 2016). In the realm of spectroscopy, the tunable nature of Dirac terahertz magneto-plasmons in graphene has been revealed, adding another layer to its multifaceted capabilities (Yan et al., 2012). Moreover, graphene mode-locked ultrafast lasers have demonstrated exceptional performance, underscoring graphene's role in advancing optical communication technologies (Sun et al., 2010).

Previous studies and developments in graphene-based optical modulators have demonstrated their potential in various applications. For instance, Liu et al. (2011) developed a broadband optical modulator using graphene, showcasing its capability to modulate light across a wide range of wavelengths. This study highlighted graphene's unique ability to achieve high modulation efficiency and speed, far surpassing traditional materials. Phare et al. (2015) further advanced the field by demonstrating a graphene electro-optic modulator with a bandwidth of 30 GHz, significantly higher than many conventional modulators. This development underscored graphene's potential for high-speed data communication. Additionally, research by Koester and Li (2012) explored waveguide-coupled graphene optoelectronics, providing insights into integrating graphene with existing optical systems to enhance their performance. These studies collectively illustrate the transformative potential of graphene in photonics, paving the way for the development of next-generation optical modulators that are faster, more efficient, and highly adaptable to various technological requirements.

2.3   Theoretical Models and Simulation Techniques

Theoretical modeling and simulation techniques play a pivotal role in advancing our understanding and application of graphene-based devices. Advanced numerical methods such as the mixed finite element method (FEM), mixed spectral element method (SEM), and discontinuous Galerkin time-domain (DGTD) methods are crucial for simulating the electromagnetic field effects of graphene, using equivalent boundary conditions like impedance transmission and surface current boundary conditions to accurately capture the complex interactions between graphene and electromagnetic fields (Gong & Liu, 2023). These sophisticated methods allow researchers to model the behavior of graphene under various conditions, improving device performance predictions. Furthermore, finite element modeling has been applied to the micro-machining of graphene-reinforced aluminum composites, revealing significant insights into the mechanical

properties and stress distribution within these materials (Bisht et al., 2017). In another study, the finite element method was used to simulate the dynamic contact effects on graphene nanoelectromechanical systems (NEMS), providing valuable data on device performance and reliability (Liu et al., 2018). Additionally, the theoretical modeling and numerical simulation of graphene growth under plasma conditions have enhanced our understanding of the material's structural and electronic properties, crucial for optimizing production techniques (Cojocaru et al., 2023). Lastly, simulations of deformation and fracture in graphene-reinforced composites have provided critical insights into the material's mechanical robustness and potential applications in high-stress environments (Song et al., 2020). These advanced simulation techniques collectively enhance the design and application of graphene-based technologies across various fields.

Theoretical models for graphene conductivity are critical for understanding and predicting the behavior of graphene-based optical modulators. One of the fundamental models used to describe graphene's conductivity is the Drude model, which accounts for the intraband conductivity of graphene by considering the motion of charge carriers under an electric field. This model is particularly useful for low-frequency applications. However, for higher frequencies, including terahertz and optical ranges, the Drude model is often combined with the interband transition model to accurately represent the full spectrum of graphene's conductivity. The Kubo formula is another widely used theoretical framework, providing a more comprehensive description by incorporating both intraband and interband contributions. This formula is essential for capturing the dynamic response of graphene under varying electric fields and frequencies, thus offering insights into its broadband optical properties (Hanson, 2008; Falkovsky & Varlamov, 2007).

Simulation techniques play a crucial role in studying optical modulators and validating theoretical models. The Finite-Difference Time-Domain (FDTD) method is one of the most used techniques due to its ability to model the time-dependent behavior of electromagnetic fields in complex structures. FDTD simulations involve discretizing both time and space to solve Maxwell's equations iteratively, making it possible to analyze the interaction of light with graphene layers and other components of the optical modulator. This method allows for detailed visualization of the electric and magnetic field distributions, providing insights into the modulator's performance and potential areas for optimization (Taflove & Hagness, 2005). Additionally, methods such as the

Finite Element Method (FEM) and Transfer Matrix Method (TMM) are also employed to model optical modulators. FEM is particularly useful for solving complex geometries and boundary conditions by breaking down the structure into smaller elements, while TMM is advantageous for analyzing layered structures and understanding the transmission and reflection properties of the modulator (Jin, 2014).

These theoretical models and simulation techniques collectively contribute to a deeper understanding of graphene's role in optical modulation, enabling the design and optimization of high-performance graphene-based optical modulators for advanced photonic applications.

CHAPTER: 3　　　METHODOLOGY

This chapter provides a detailed explanation of the MATLAB code used for the simulation of optical waveguides with graphene-based optical modulators. It includes a description of the key functions and scripts used in the simulation, highlighting their roles and interactions within the overall code structure.

3.1　Code Structure Overview

The MATLAB code for the FDTD simulation of graphene-based optical modulators is organized into several sections, each handling different aspects of the simulation. The main components of the code structure are:
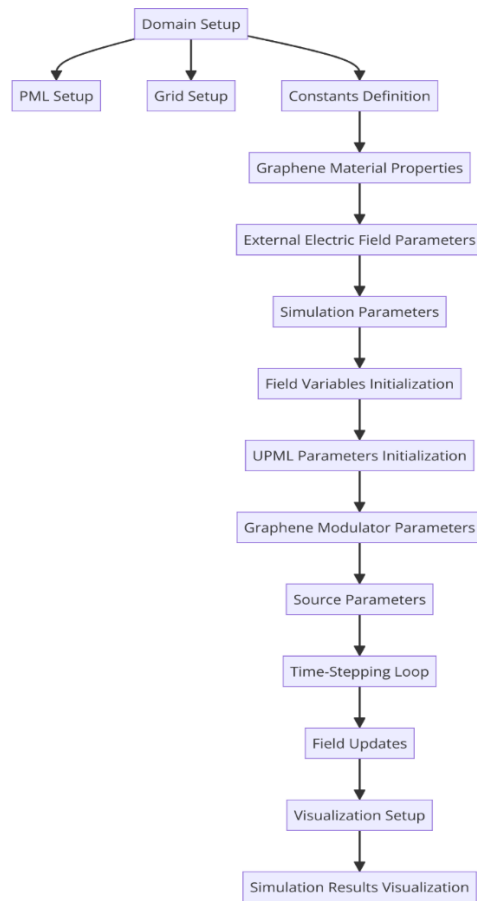
Figure 3.1: Flow chart representing code structure.

1. Initialization: Setting up the simulation parameters, including domain size, grid resolution, material properties, and boundary conditions.

2. Field Variables Initialization: Initializing the electric and magnetic field components and PML layers.

3. Graphene Modulator Parameters: Defining the properties of the graphene modulator, including conductivity, refractive index, and source parameters.

4. Simulation Loop: Iteratively updating the electric and magnetic fields over time, injecting the source signal, and recording data.

5. Post-Processing: Analyzing and visualizing the results of the simulation.

3.2 Finite-Difference Time-Domain (FDTD) Method

3.2.1 Explanation of the FDTD Method and its Application in the Simulation

The Finite-Difference Time-Domain (FDTD) method is a powerful numerical technique used to solve Maxwell's equations for complex electromagnetic problems. It is particularly well-suited for modeling the interaction of light with materials and structures, such as waveguides, metamaterials, and photonic devices. The FDTD method discretizes both time and space, allowing for the direct simulation of the time-dependent behavior of electromagnetic fields.

3.2.2 Fundamentals of the FDTD Method

Maxwell's equations describe the behavior of electric and magnetic fields:

1. Faraday's Law:

$$\nabla \times E = -\frac{\partial B}{\partial t} \quad \ldots\ldots\ldots\ldots\ldots\ldots\ldots \quad (1)$$

2. Ampère's Law (with Maxwell's correction):

$$\nabla \times H = \frac{\partial D}{\partial t} + J \ldots\ldots\ldots\ldots\ldots\ldots\ldots \quad (2)$$

3. Gauss's Law for Electricity:

$$\nabla \cdot D = \rho \ldots\ldots\ldots\ldots\ldots\ldots.\ldots\ldots \quad (3)$$

4. Gauss's Law for Magnetism:

$$\nabla \cdot B = 0 \ldots\ldots\ldots\ldots\ldots\ldots.\ldots\ldots \quad (4)$$

In the FDTD method, these equations are discretized using central-difference approximations for both time and space derivatives. The spatial domain is divided into a grid of cells, and time is divided into discrete steps. The electric field E and magnetic field H are calculated at alternating half-time steps, which is known as the leapfrog scheme.

The update equations for the electric and magnetic fields in one dimension are given by:

$$E_i^{n+1} = E_i^n + \frac{\Delta t}{\epsilon} \left(\frac{H_{i+\frac{1}{2}}^{n+\frac{1}{2}} - H_{i-\frac{1}{2}}^{n+\frac{1}{2}}}{\Delta x} - J_i^{n+\frac{1}{2}} \right) \dots\dots\dots\dots\dots\dots \text{(5)}$$

$$H_{i+\frac{1}{2}}^{n+\frac{1}{2}} = H_{i+\frac{1}{2}}^{n-\frac{1}{2}} + \frac{\Delta t}{\epsilon} \left(\frac{E_{i+1}^n - E_i^n}{\Delta x} \right) \dots\dots\dots\dots\dots\dots\dots\dots \text{(6)}$$

where Δt and Δx are the time step and spatial step sizes, respectively, and ϵ and μ are the permittivity and permeability of the medium.

3.3 Simulation Domain and Grid Setup

The simulation domain for this study is designed to accurately model the behavior of a graphene-based optical modulator within a finite space. The domain dimensions are defined to be Lx=20 units and Ly=20 units in the x and y directions, respectively. This choice of dimensions ensures that the domain is large enough to capture the essential interactions within the modulator while maintaining computational efficiency. The grid resolution is set at dx=0.2 units, which is also used for dy to ensure isotropic resolution, resulting in nx= (fix Lx/dx) grid points in the x direction and ny= (fix Ly/dy) grid points in the y direction.

To absorb any outgoing waves and prevent reflections that could interfere with the simulation, Perfectly Matched Layer (PML) regions are included at the boundaries of the simulation domain. The PML thickness is set to 20 grid points, expanding the grid to nx_pml= nx+2*PML thickness and ny_pml= ny+2*PML thickness. Additionally, the substrate, modeled as silicon dioxide (SiO2) with a refractive index of 1.45, is included to account for its effects on the optical modulator. The substrate thickness is defined as 2 grid points.
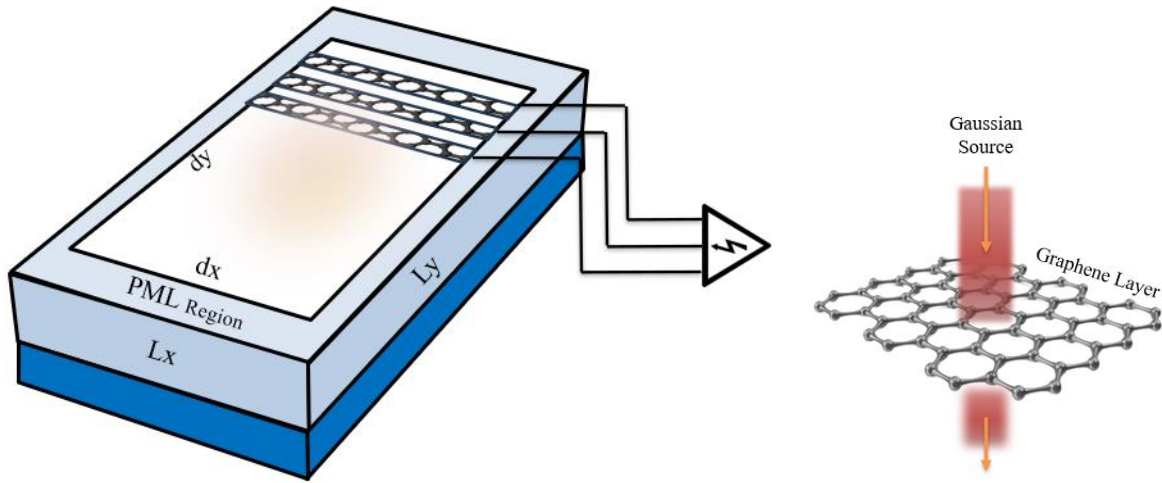
Figure 3.2: Schematic of the simulation domain for the graphene-based optical modulator showing the grid setup and PML regions.

The x and y axes are represented as linear spaces including the PML regions, resulting in x= linspace (0, Lx, nx_pml) and y= linspace (0, Ly, ny_pml). This setup ensures that the entire domain, including the active region and the boundary layers, is accurately represented for the simulations. By carefully defining these parameters, the simulation domain is optimized to study the interaction between the optical field and the graphene modulator, capturing the essential physics while maintaining computational feasibility.

3.4 Time Stepping and Stability Criteria

The time domain setup and stability criteria are crucial for ensuring accurate and stable Finite-Difference Time-Domain (FDTD) simulations. In this study, the total simulation time is set to T=10 units. The time step dt is determined based on the Courant stability condition, which is necessary to ensure the numerical stability of the FDTD method. The Courant condition for a 2D FDTD simulation is given by:

$$\text{dt} \leq \frac{dx}{c\sqrt{2}} \quad \text{.................} \quad (7)$$

where ccc is the speed of light in vacuum and dx is the spatial grid resolution. For this simulation, dx=0.2 units, and c= 3 x 10^8 m/s, resulting in:

$$dt = 0.5 \text{ x } \frac{dx}{c*2^{0.25}} \dots\dots\dots\dots\dots\dots \text{ (8)}$$

This time step ensures that the simulation remains stable and accurate throughout the entire domain.

Custom intervals are defined for specific calculations to optimize the computational efficiency and focus on the critical aspects of the simulation. For example, the interval for updating the graphene conductivity and external electric field parameters is set to 10×dt. This interval allows for the capture of dynamic changes in the modulator's properties without the need for excessive computations at every time step.

By carefully setting up the time domain and adhering to the stability criteria, the simulation can accurately model the interactions within the graphene-based optical modulator. This approach ensures that the results are both reliable and computationally efficient, providing valuable insights into the performance and optimization of the modulator.

3.5   Material Properties

3.5.1   Physical Constants and Graphene Material Properties

To accurately simulate the behavior of the graphene-based optical modulator, it is essential to incorporate the correct physical constants and material properties. The key physical constants used in this simulation include:

- **Permittivity of Free Space ($\epsilon 0$)**: $8.854187817 \times 10^{-12}$ F/m

- **Speed of Light in Vacuum (c)**: 3×10^8 m/s

Graphene's unique properties are central to its effectiveness in optical modulation. The graphene layer is modeled with the following parameters:

- **Graphene Thickness**: 0.34×10^{-6} meters

- **Carrier Concentration**: 5×10^{16} m^{-2} (increased to enhance modulation performance)

- **Mobility**: 1 $m^2/$ (V·s) (increased to reflect high-quality graphene samples)

- **Temperature**: 300 K

The conductivity of graphene, which is crucial for its modulation capability, is dynamically calculated based on the applied voltage and the material's intrinsic properties using the Drude model and related equations.

3.5.2 Parameters for the External Electric Field and Applied Voltage

The performance of the graphene-based optical modulator is heavily influenced by the external electric field and the applied voltage. These parameters are defined as follows:

- **Applied Voltage Amplitude (V_O)**: 5.0 V (increased for higher modulation efficiency)

- **Voltage Frequency ($V_{frequency}$)**: 1×10^{12} Hz

The external electric field, which interacts with the graphene layer to achieve modulation, is characterized by:

- **Maximum Electric Field Strength (E_{field_max})**: 1×10^5 V/m

- **Electric Field Frequency (E_{field_freq})**: 1×10^{12} Hz

These parameters are critical for determining the modulation efficiency and the overall performance of the optical modulator. The external electric field's influence on the refractive index of the waveguide material and the dynamic tuning of the graphene's optical properties are key factors in achieving effective modulation. By carefully defining and integrating these material properties and external parameters, the simulation provides a comprehensive analysis of the graphene-based optical modulator's capabilities and potential for high-speed optical communication applications.

3.6 Initialization of Field Variables

3.6.1 Initial Conditions for Electric and Magnetic Fields

In the simulation of the graphene-based optical modulator, the initial conditions for the electric and magnetic fields are critical for accurate modeling. The electric field component E_z and the magnetic field components H_x and H_y are initialized to zero across the entire simulation domain. This setup ensures a controlled starting point for observing the evolution of these fields under the influence of the applied voltage and external electric field.

$E_z(x, y): 0$ for all (x, y) …………………… (9)

$H_x(x, y): 0$ for all (x, y) …………………… (10)

$H_y(x, y): 0$ for all (x, y) …………………… (11)

To account for the presence of the substrate, the electric field E_z is adjusted within the substrate region by multiplying it by the substrate's refractive index (1.45 for SiO2). This adjustment ensures that the initial conditions reflect the physical properties of the substrate material.

3.6.2 PML Conductivity Profiles and Graphene Modulator Parameters

Perfectly Matched Layer (PML) regions are implemented to absorb outgoing waves and prevent reflections from the boundaries of the simulation domain. The PML conductivity profiles for both x and y directions are crucial for the effectiveness of these layers. The maximum conductivity σ_{max} for the PML regions is set to 0.15. The conductivity profiles are defined using a polynomial grading, which gradually increases the conductivity towards the edges of the simulation domain, ensuring smooth absorption of outgoing waves.

$$\sigma_x(i) = \sigma_{max}\left(\frac{i}{PML\ thickness}\right)^4 \quad \text{for i=1, 2, 3, ……., PML thickness} \dots\dots\dots\dots\dots\dots (12)$$

$$\sigma_y(i) = \sigma_x(i) \dots\dots\dots\dots\dots\dots\dots\dots\dots\dots\dots\dots\dots\dots\dots\dots\dots\dots\dots\dots\dots\dots\dots\dots\dots\dots (13)$$

$$\sigma_x\left(nx_{pml} - i + 1\right) = \sigma_x(i) \dots\dots\dots\dots\dots\dots\dots\dots\dots\dots\dots\dots\dots\dots\dots\dots\dots\dots\dots\dots (14)$$

$$\sigma_y\left(ny_{pml} - i + 1\right) = \sigma_y(i) \dots\dots\dots\dots\dots\dots\dots\dots\dots\dots\dots\dots\dots\dots\dots\dots\dots\dots\dots\dots (15)$$

These profiles ensure that the PML regions effectively attenuate the waves without causing reflections that could interfere with the simulation.

For the graphene modulator, specific parameters are defined to accurately represent its properties and behavior in the simulation. The initial conductivity of the graphene modulator $\sigma_{modulator}$ is set to 0.02 S/m. The locations and lengths of the graphene layers within the simulation domain are specified, ensuring that the graphene's influence on the optical fields is appropriately modeled.

The graphene layers are positioned as follows:

Layer 1: (x =round ($nx_{pml}/4$), y=PML thickness +round (ny/4)) with length 20 units

Layer 2: (x =round ($nx_{pml}/4$)+2, y=PML thickness +round (ny/4)) with length 20 units

Layer 3: (x =round ($nx_{pml}/4$)+4, y=PML thickness +round (ny/4)) with length 20 units

These parameters ensure that the graphene layers are correctly incorporated into the simulation, allowing for an accurate analysis of their impact on the optical modulator's performance. By carefully initializing the field variables and defining the PML and graphene parameters, the simulation can accurately model the dynamic behavior of the graphene-based optical modulator.

3.7 Source Parameters

The source in the simulation is designed to generate a Gaussian pulse, which is a widely used waveform in optical simulations due to its smooth temporal and spectral characteristics. The Gaussian pulse is characterized by its central frequency, pulse width, and time delay, ensuring a well-defined shape and timing for precise interaction with the graphene-based optical modulator. The central frequency of the Gaussian pulse is set to 1×10^{12} Hz (1 THz), aligning with the operational range of the modulator and allowing exploration of its performance in the terahertz regime. The pulse width, τ, is determined by the inverse of the central frequency, resulting in a pulse width of 1×10^{-12} seconds (1 picosecond). This short pulse width ensures that the pulse can resolve the fast dynamics of the modulator effectively.

To isolate the effects of the Gaussian pulse from any initial conditions or boundary effects in the simulation, a time delay, t0, is set to 5τ, equating to 5×10^{-12} seconds. This delay allows the pulse to reach its peak after the initial transients in the simulation have settled. The source is positioned at the center of the simulation domain to ensure symmetric propagation of the pulse through the graphene-based modulator, with the x and y coordinates of the source set to the midpoint of the simulation grid.

The electric field Ez at the source position is updated according to the Gaussian pulse equation:

$$Ez\ (x_{source}, y_{source}, t) = Ez\ (x_{source}, y_{source}, t) + \exp\left(-\frac{(t-t_0)^2}{2\tau^2}\right) \cos(2\pi f_{source}(t - t_0)) \quad \ldots\ldots\ldots(16)$$

This equation ensures the Gaussian pulse is introduced smoothly into the simulation, providing a well-defined and controlled input signal for analyzing the modulator's performance. By carefully defining these source parameters, the simulation can accurately generate and propagate the Gaussian pulse through the graphene-based optical modulator, facilitating a detailed study of the modulator's response to high-frequency optical signals.

3.8   Graphene Modulator Configuration

The configuration of the graphene modulator within the simulation domain is crucial for accurately modeling its impact on the optical fields. The graphene layers are strategically placed to interact effectively with the optical fields propagating through the waveguide. Specifically, the first graphene layer is positioned at one-quarter of the total simulation domain length in the x-direction and at a height just above the PML layer in the y-direction, extending for 20 units in length. The second layer is similarly positioned but shifted slightly to ensure a small separation from the first layer, maintaining the same length and y-position. The third layer follows the same pattern, ensuring an equal spacing between the graphene layers. These positions ensure that the graphene layers are evenly spaced and can modulate the optical signal efficiently.

The dynamic calculation of graphene's conductivity at each time step is a critical aspect of the simulation. The conductivity $\sigma_{graphene}$ is influenced by the applied voltage, temperature, carrier concentration, and mobility of the graphene. The applied voltage V(t) varies sinusoidally over time, with its value at each time step given by V(t)=$V_O$sin($2\pi f_{voltage}$t), where V_O is the amplitude of the applied voltage and $f_{voltage}$ is its frequency. Using this voltage, the graphene conductivity is calculated using the Drude model:

$$\sigma_{graphene} = q \cdot n \cdot \mu \ldots\ldots\ldots\ldots\ldots\ldots\ldots\ldots\ldots\ldots\ldots..(17)$$

where n is the carrier concentration, q is the elementary charge, and μ is the mobility. This dynamic calculation ensures that the simulation accurately reflects the modulator's behavior as the applied voltage changes, providing a realistic and detailed analysis of its performance. By carefully defining the placement and dimensions of the graphene layers and dynamically calculating their conductivity, the simulation offers valuable insights into the capabilities of the graphene-based optical modulator.

3.9   Refractive Index Calculation

The refractive index of the waveguide material is a critical factor in determining the behavior of light as it propagates through the graphene-based optical modulator. In this study, the refractive index is dynamically calculated based on the external electric field and the applied voltage, reflecting the real-time changes in the optical properties of the modulator.

The baseline refractive index of the waveguide material is set to a constant value, typically around 1.5 for standard optical materials. However, the presence of an external electric field induces changes in the refractive index, a phenomenon known as the electro-optic effect. The external electric field, which varies sinusoidally over time, affects the electron distribution in the waveguide material, leading to a change in the refractive index.

At each time step of the simulation, the current electric field is calculated based on the predefined maximum field strength and frequency. This electric field influences the refractive index, which is computed by adding a proportional change to the baseline refractive index. The change in refractive index is directly related to the strength of the electric field, ensuring that stronger fields result in more significant changes.

Additionally, the applied voltage across the graphene layers also contributes to the modulation of the refractive index. The voltage alters the carrier concentration in the graphene, which in turn affects the overall optical properties of the waveguide. The combined effect of the external electric field and the applied voltage results in a dynamic refractive index that adapts in real-time during the simulation.

By incorporating these factors, the refractive index calculation in the simulation provides a realistic and responsive model of the optical modulator's behavior. This dynamic calculation allows for precise modeling of light propagation through the modulator, accounting for the real-time changes induced by the external electric field and applied voltage. This approach ensures that the simulation accurately reflects the performance and modulation capabilities of the graphene-based optical modulator.

3.10 Calculation of Modulation Depth and Propagation Loss

Modulation depth (MD) and propagation loss (PL) are critical parameters in evaluating the performance of optical modulators. According to Zhou et al. (2022), these parameters are calculated as follows:

1. **Modulation Depth (MD)**:

$$\text{MD} = \alpha_{OFF} - \alpha_{ON} \quad \text{..........................}(18)$$

Where α_{OFF} is the optical loss per length in the "OFF" state and α_{ON} is the optical loss per length in the "ON" state.

2. **Optical Loss per Length (α)**:

$$\alpha = \frac{40\pi(log_{10}e).Img(n_{eff})}{\lambda} \quad \text{........................}(19)$$

Where λ is the wavelength of the incident light and $Img(n_{eff})$ is the imaginary component of the effective refractive index.

3. **Propagation Loss (PL)**:

$$\text{PL} = \alpha_{ON} \text{.....................................}(20)$$

These calculations provide a basis for comparing the optical modulation properties between different designs and configurations.

3.11 Visualization and Data Collection

Effective visualization and data collection methods are essential for analyzing the performance of the graphene-based optical modulator. These methods help interpret the simulation results, providing insights into the behavior of electric and magnetic fields, modulation efficiency, and beam positions. To visualize the electric (Ez) and magnetic (Hx and Hy) field distributions, 2D color plots are utilized. These plots offer snapshots of field intensities at various points within the simulation domain, using color gradients to distinguish between high and low intensities. This approach allows for an intuitive understanding of how the fields evolve over time and interact within the modulator. For the magnetic fields, quiver plots are employed to represent the field vectors, showing the direction and magnitude of Hx and Hy components. Quiver plots are

particularly useful for identifying complex magnetic field behaviors such as vortices and field lines.

Dynamic visualization is achieved by generating a series of plots at different time steps, allowing the observation of the temporal behavior of the fields. This includes the propagation of pulses, reflections, and interactions with the graphene layers. By animating these sequences, one can observe real-time effects of modulation and the influence of external electric fields and applied voltage.

Data collection focuses on key performance metrics such as modulation efficiency and beam positions. Modulation efficiency is tracked by monitoring the peak electric field (Ez) at each time step and comparing maximum field values before and after modulation. This provides a measure of the modulator's effectiveness. Beam positions are recorded at regular intervals to capture the trajectory of the optical beam within the waveguide, helping analyze beam steering, focusing, and potential losses or distortions introduced by the modulator. Additionally, comprehensive time series data for electric and magnetic fields, applied voltage, and external electric field are recorded to facilitate detailed post-processing analysis. This includes Fourier transforms to study frequency components and temporal analysis to investigate dynamic behaviors.

By employing these visualization and data collection methods, the simulation provides a thorough analysis of the graphene-based optical modulator's performance. These techniques enable a detailed understanding of field distributions, modulation efficiency, and beam dynamics, offering valuable insights into the design and optimization of advanced optical modulators.

CHAPTER: 4   RESULTS AND DISCUSSION

4.1   Electric and Magnetic Field Distributions

4.1.1   Analysis of Electric Field (Ez) Distribution Over Time

The analysis of the electric field Ez distribution over time provides crucial insights into the behavior and performance of the graphene-based optical modulator. The evolution of Ez is governed by Maxwell's equations, which in two dimensions (2D) for the zzz-component of the electric field can be expressed as:

$$\frac{\partial Ez}{\partial t} = (\frac{1}{\epsilon}\frac{\partial Hy}{\partial x} - \frac{\partial Hx}{\partial y}) - \sigma Ez \ldots\ldots\ldots\ldots\ldots\ldots\ldots\ldots\ldots\ldots\ldots(21)$$

where ϵ is the permittivity of the medium, Hx and Hy are the magnetic field components, and σ is the conductivity of the material (graphene, in this case).
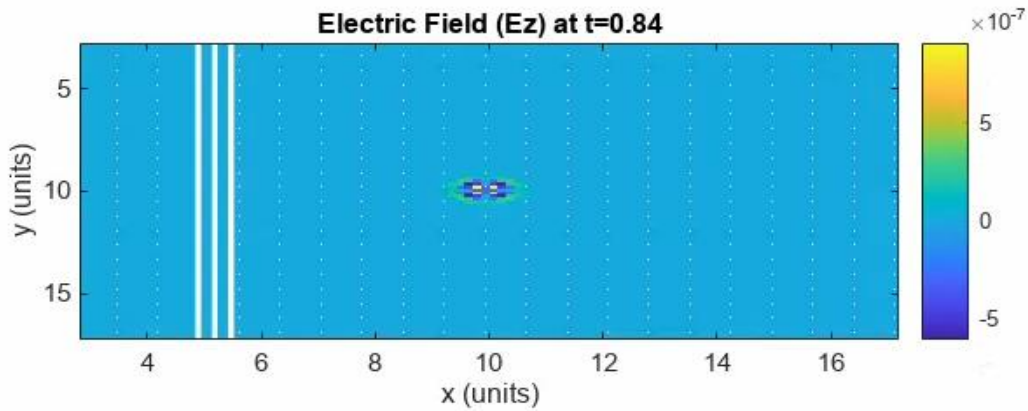

Figure 4.1: Electric Field (Ez) at t=0.84
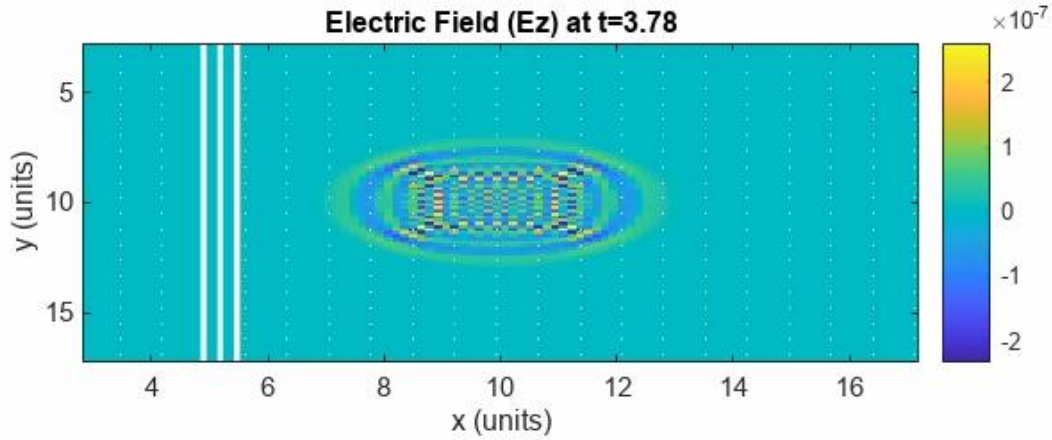
Figure 4.2: Electric Field (Ez) at t=3.78
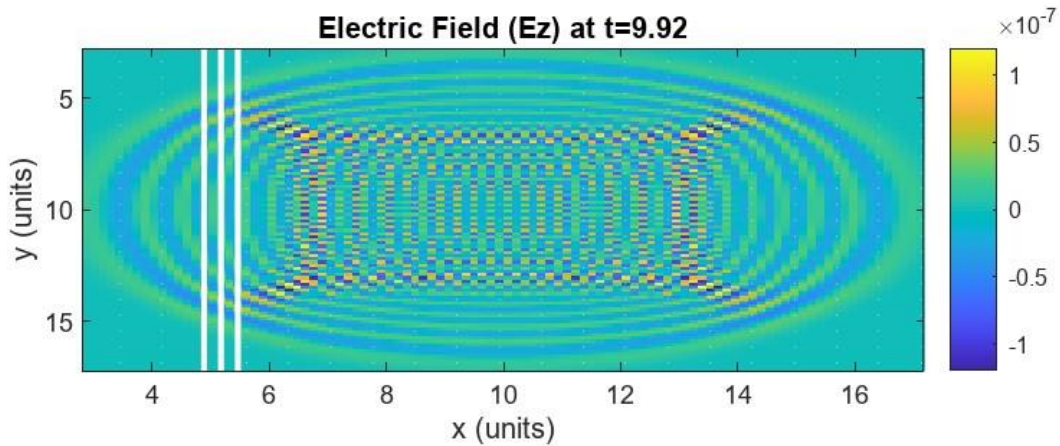
Figure 4.3: Electric Field (Ez) at t=9.92

Initially, Ez is set to zero, allowing the influence of the applied voltage and external electric field to be clearly observed. As the simulation progresses, the intensity and distribution of Ez change, revealing the interaction of the optical signal with the graphene layers. Snapshots of the Ez field distribution at each time step illustrate how the electric field propagates and is modulated. These snapshots highlight regions of high field concentration, indicating significant modulation effects.

The applied voltage V(t) varies sinusoidally and is given by:

$$V(t) = V_O \sin(2\pi f_{voltage} t) \quad \ldots\ldots\ldots\ldots\ldots\ldots\ldots\ldots\ldots\ldots\ldots\ldots\ldots\ldots\ldots\ldots(22)$$

where V_O is the amplitude and $f_{voltage}$ is the frequency of the applied voltage. This voltage affects the graphene's conductivity, dynamically altering the Ez field.

and refractive index.

Comparison of Field Values Before and After Modulation

To evaluate the effectiveness of the graphene-based optical modulator, we compare the electric field distributions before and after the modulation is applied. This involves analyzing the field distributions at different stages of the simulation, particularly before the voltage is applied and after the voltage reaches its peak.

Before Modulation

Before the modulation is applied, the electric field propagates through the waveguide without significant interaction with the graphene layer. The following plot shows the Ez distribution early step before the voltage is applied.
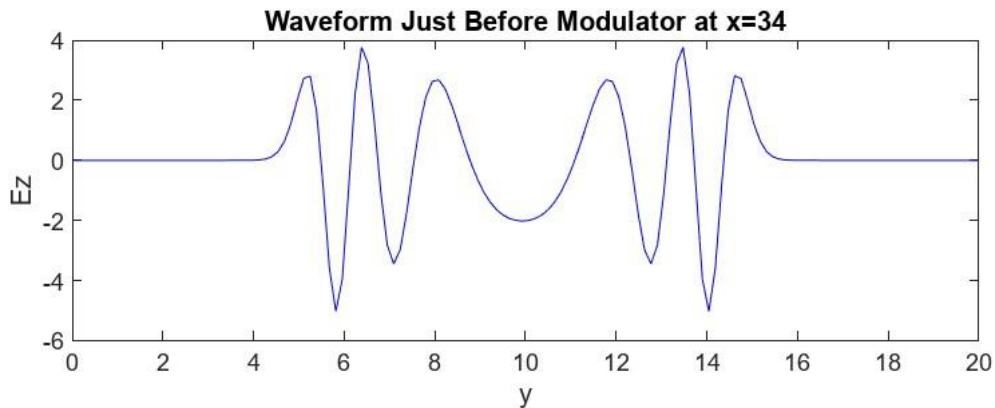

Figure 4.4: Waveform Just Before Modulator at x=34

After Modulation

After the modulation is applied, the electric field interacts with the graphene layer, resulting in changes to its amplitude and phase. The following plot shows the Ez distribution later step after the voltage has been applied.
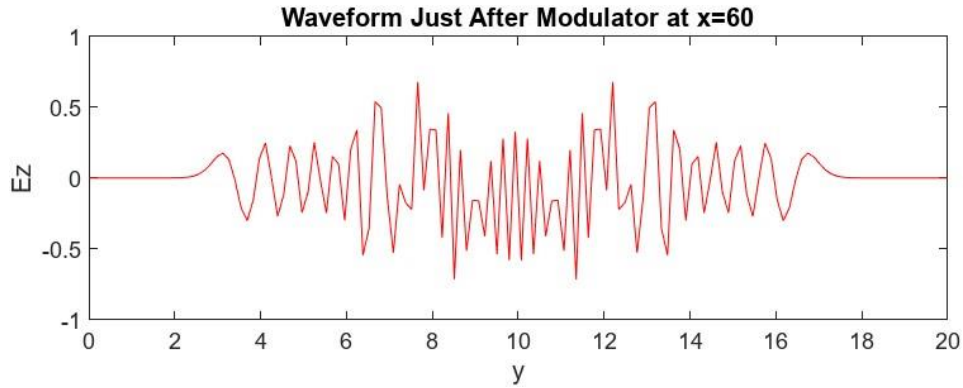
Figure 4.5: Waveform Just After Modulator at x=60

Comparison and Discussion

By comparing the field distributions before and after modulation, we can observe the effects of the graphene modulator. Key points of comparison include:

1. **Field Amplitude**: Changes in the amplitude of the Ez field indicate modulation effects. An increase or decrease in field intensity at certain locations signifies the influence of the applied voltage on the graphene's conductivity.

2. **Phase Shifts**: Any phase shifts observed in the field distribution are indicative of changes in the refractive index of the graphene layer. This is a direct result of the applied voltage and its effect on the carrier concentration in graphene.

3. **Field Distribution**: The overall distribution of the Ez field may change due to the modulation, with potential shifts in the field patterns and propagation characteristics.

The results of this analysis provide valuable insights into the performance of the graphene-based optical modulator. By understanding how the modulator affects the electric field distribution, we can optimize the design and operation of the device for various applications in optical communication and photonics.

4.1.2   Electric Field and Refractive Index

This section focuses on the relationship between the electric field strength and the refractive index over time. The graph below illustrates how the refractive index changes in response to the varying electric field strength, highlighting the dynamic interaction between the applied voltage and the optical properties of the graphene-based modulator.
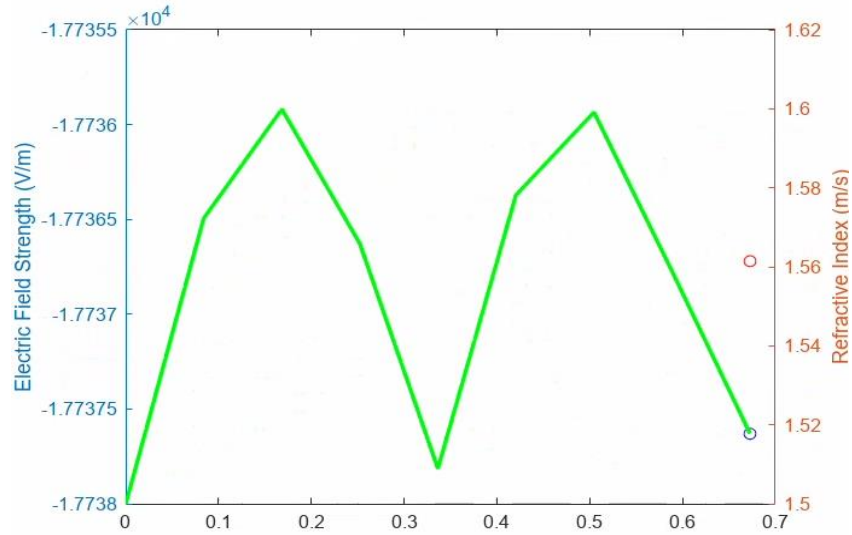
Figure 4.6: graph showing electric strength and reflective index at 0.68s
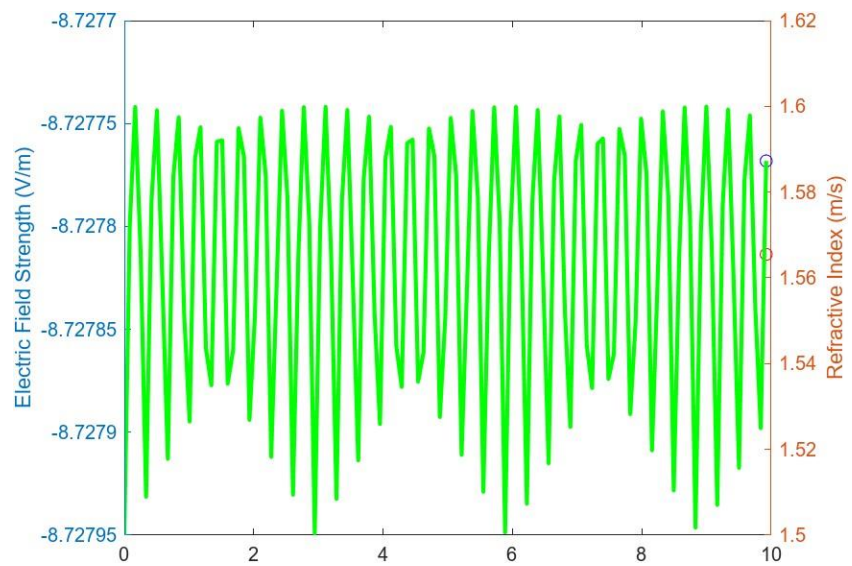
Figure 4.7: graph showing electric strength and reflective index at 10s

The graph shows that as the electric field strength varies, the refractive index also fluctuates, indicating the effectiveness of the modulation process. This dynamic visualization provides valuable insights into the performance and optimization of the graphene-based optical modulator.

Visualization of Magnetic Fields (Hx, Hy) Before and After Modulation

The visualization of magnetic fields Hx and Hy provides complementary information to the electric field analysis, offering a complete picture of the electromagnetic behavior within the modulator. The magnetic fields are governed by Maxwell's curl equations, which in 2D can be expressed as:

$$\frac{\partial Hx}{\partial t} = -\frac{1}{\mu}\frac{\partial Ez}{\partial y} \dots\dots\dots\dots\dots\dots\dots\dots\dots\dots\dots\dots\dots\dots\dots\dots\dots\dots\dots(23)$$

$$\frac{\partial Hy}{\partial t} = \frac{1}{\mu}\frac{\partial Ez}{\partial x}\dots\dots\dots\dots\dots\dots\dots\dots\dots\dots\dots\dots\dots\dots\dots\dots\dots\dots(24)$$

where μ is the permeability of the medium.

Figure 4.8: Magnetic Field (Hx,Hy) at x= 0.82

Figure 4.9: Magnetic Field (Hx,Hy) at x= 5.42
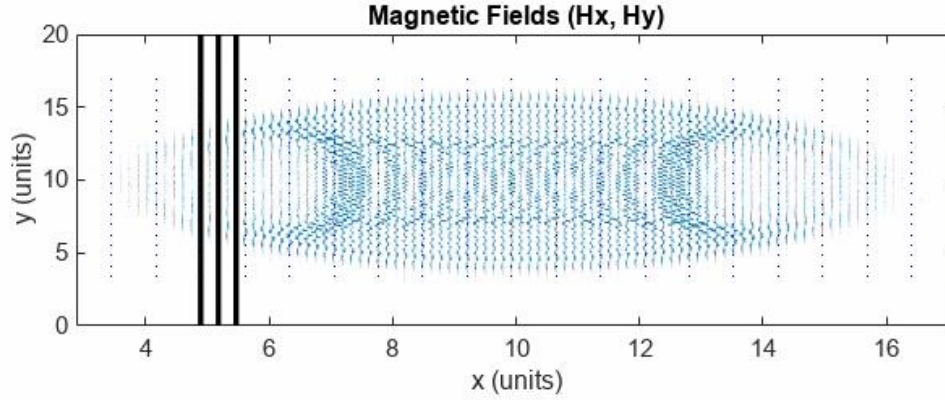
Figure 4.10: Magnetic Field (Hx,Hy) at x= 8.94

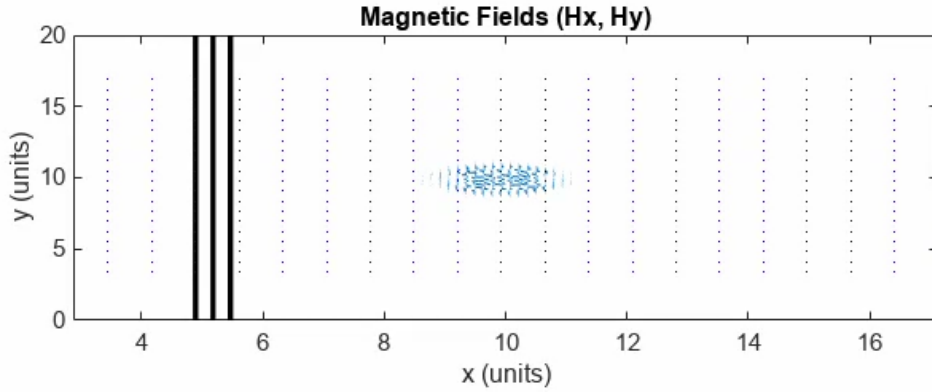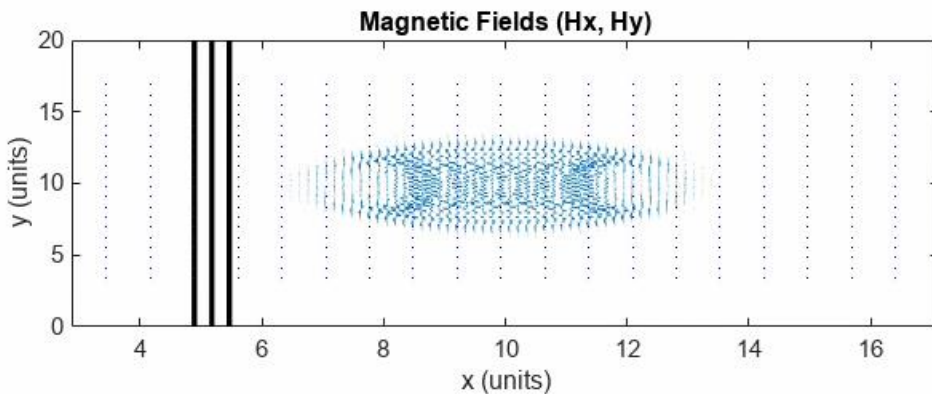Before modulation, the magnetic fields are relatively uniform, with vectors pointing in consistent directions according to the initial conditions and the external electric field. As modulation begins, the magnetic fields start to change in direction and intensity, reflecting the interaction with the dynamically changing electric field and the modulating influence of the graphene layers. After modulation, the quiver plots of Hx and Hy show altered patterns, indicating the effects of the applied voltage and external electric field on the electromagnetic field distribution.

By visualizing the magnetic fields before and after modulation, the impact of the modulation process on electromagnetic wave propagation can be observed. This visualization, combined with the electric field analysis, helps identify key areas where the fields are most affected, providing insights into the efficiency and effectiveness of the graphene-based modulator. The comprehensive understanding gained from these analyses enables the optimization of design parameters for improved modulation efficiency and overall functionality of the optical modulator.

4.1.3 Analysis of Magnetic Field Waveforms Before and After Modulation

To evaluate the effect of the graphene modulator on the magnetic fields, we analyze the Hx and Hy waveforms before and after modulation. This involves comparing the field distributions and waveforms at different stages of the simulation.

Before Modulation

Before the modulation is applied, the magnetic fields propagate through the waveguide without significant interaction with the graphene layer. The following plots show the Hx and Hy distributions early step before the voltage is applied.
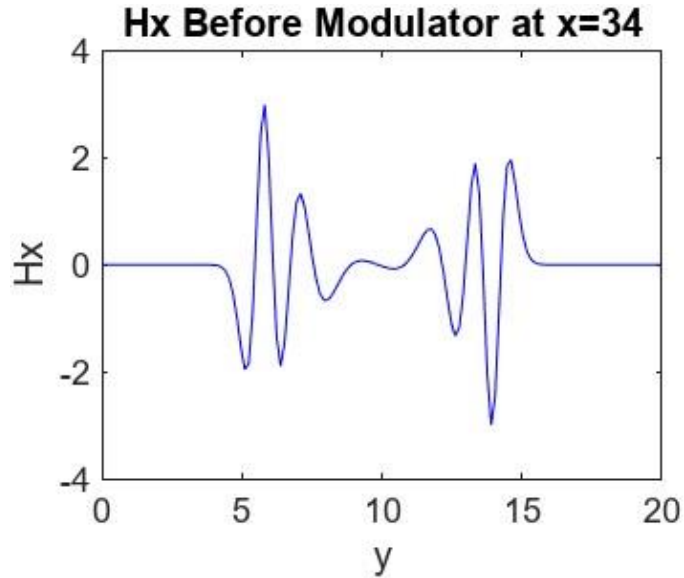
Figure 4.11: Waveform Hx before modulator at x=34

Figure 4.12: Waveform Hy before modulator at x=34

After Modulation

After the modulation is applied, the magnetic fields interact with the graphene layer, resulting in changes to their amplitude and phase. The following plots show the Hx and Hy distributions later step after the voltage has been applied.
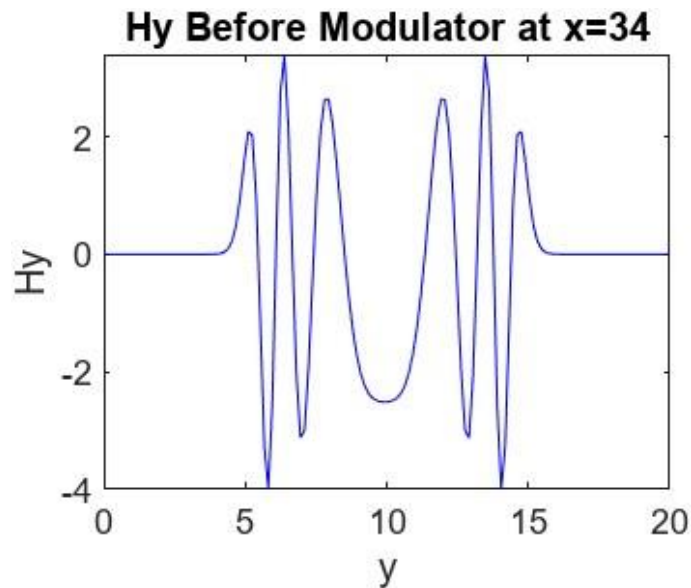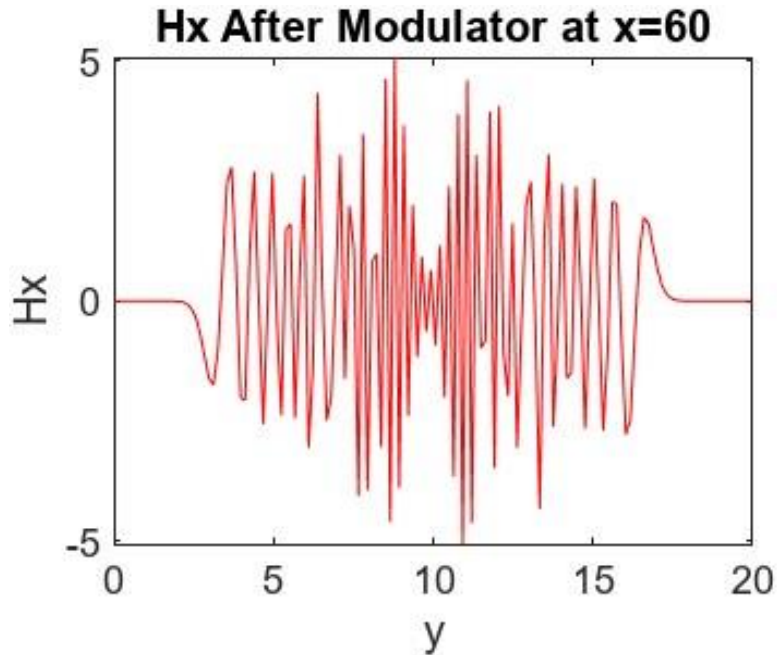

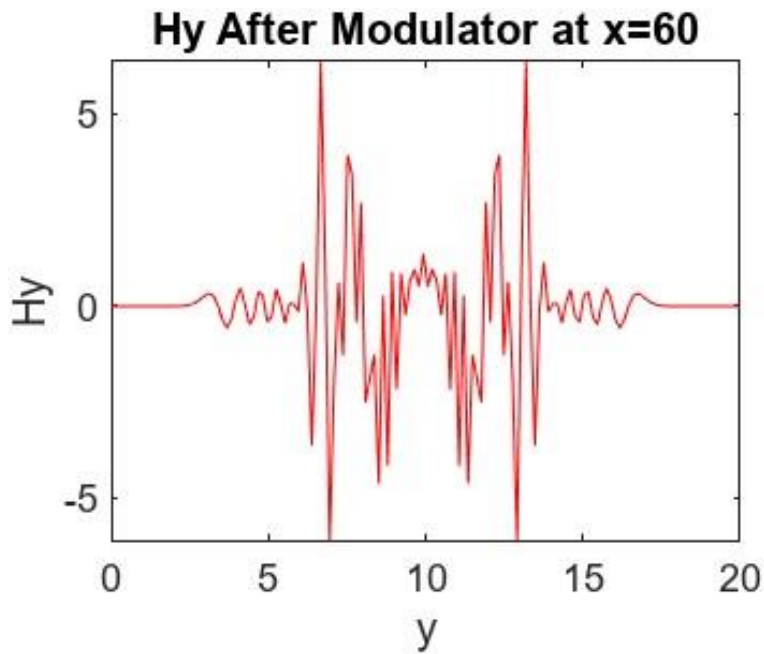*Figure 4.13: Waveform Hx After modulator at x=60*

Figure 4.14: Waveform Hy After modulator at x=60

Comparison and Discussion

By comparing the magnetic field distributions before and after modulation, we can observe the effects of the graphene modulator. Key points of comparison include:

1. **Field Amplitude**: Changes in the amplitude of the Hx and Hy fields indicate modulation effects. An increase or decrease in field intensity at certain locations signifies the influence of the applied voltage on the graphene's conductivity.

2. **Phase Shifts**: Phase shifts in the magnetic fields can be observed by comparing the field distributions at different time steps. These shifts are indicative of changes in the refractive index due to the applied voltage.

3. **Field Distribution**: The overall distribution of the Hx and Hy fields may change due to the modulation, with potential shifts in the field patterns and propagation characteristics.

The results of this analysis provide valuable insights into the performance of the graphene-based optical modulator. By understanding how the modulator affects the magnetic field distribution, we can optimize the design and operation of the device for various applications in optical communication and photonics.

4.2   Modulation Efficiency

4.2.1   Calculation of Modulation Efficiency at Different Time Steps

Modulation efficiency is a key performance metric for the graphene-based optical modulator, reflecting its ability to effectively alter the optical signal. The code calculates modulation efficiency dynamically at each time step, providing insights into the modulator's performance over time. The modulation efficiency η is determined by considering the conductivity of the graphene modulator and the applied voltage.

The modulation efficiency can be expressed as:

$$\eta(t) = \sigma_{modulator} \times |V(t)| \dots\dots\dots\dots\dots\dots\dots\dots\dots\dots\dots\dots\dots\dots\dots\dots\dots\dots\dots(25)$$

where:

- $\sigma_{modulator}$ is the conductivity of the graphene modulator,

- V(t) is the applied voltage at time t.

The applied voltage V(t) varies sinusoidally, given by:

$$V(t) = V_O \sin(2\pi f_{voltage} t) \dots\dots\dots\dots\dots\dots\dots\dots\dots\dots\dots\dots\dots\dots\dots\dots\dots\dots\dots\dots\dots\dots(26)$$

where:

- V_O is the amplitude of the applied voltage,

- $f_{voltage}$ is the frequency of the applied voltage.

During the simulation, the peak electric field Ez is monitored, and the modulation efficiency is calculated by comparing the maximum electric field values before and after modulation. This provides a time series of efficiency values, allowing for an analysis of how efficiently the graphene-based modulator operates over time. The following figure illustrates the modulation efficiency over time, showing fluctuations that correspond to the dynamic changes in the applied voltage and electric field.
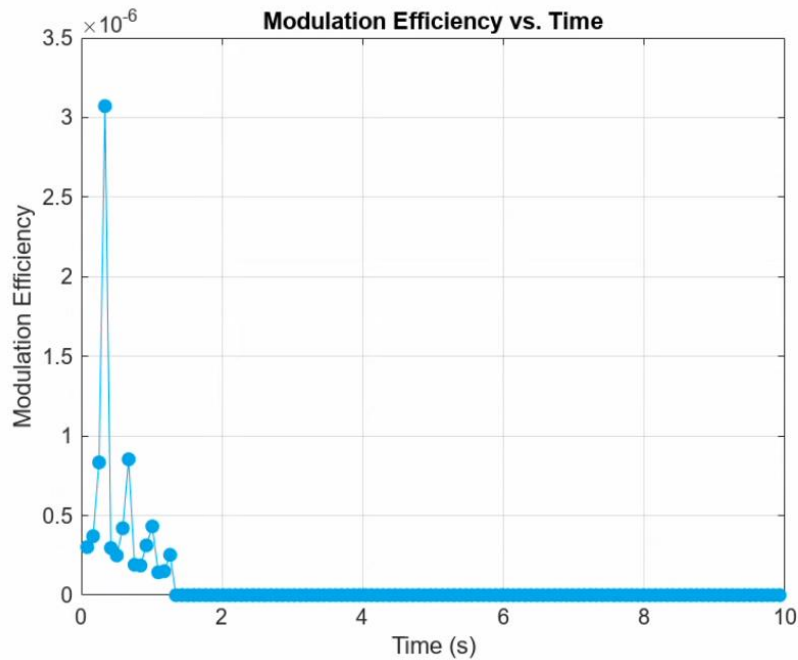
Figure 4.15: Time-Dependent Modulation Efficiency of Graphene-Based Optical Modulator
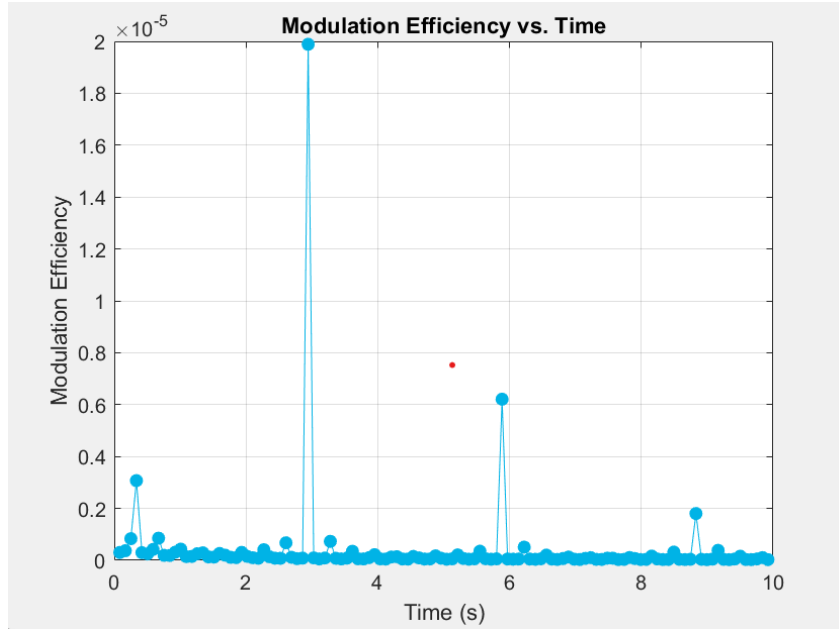
Figure 4.16: Modulation Efficiency of Graphene-Based Optical Modulator Over Time

The voltage applied over time is crucial for understanding the dynamics of the modulation process. The following figure shows the voltage over time used in the simulation, along with the relevant simulation parameters such as time, temperature, carrier concentration, mobility, and the current voltage value.
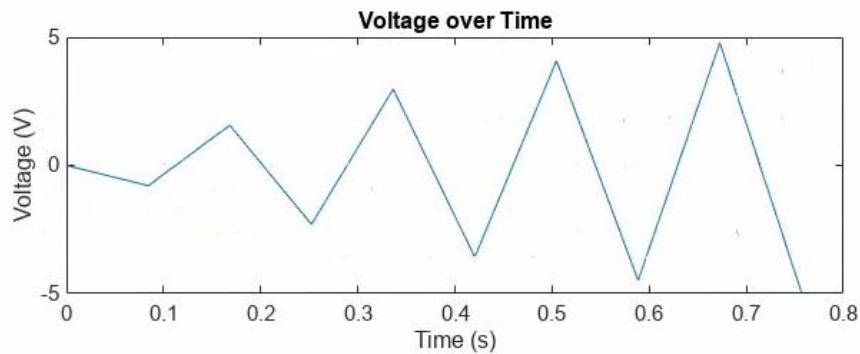
Time: 0.76 s
Temp: 300.00 K
Carrier Conc.: 5.00e+16 m⁻2
Mobility: 1.00 m^2/(V*s)
Current Voltage: -4.95 V

Figure 4.17: Graph of Voltage over time at 0.76s
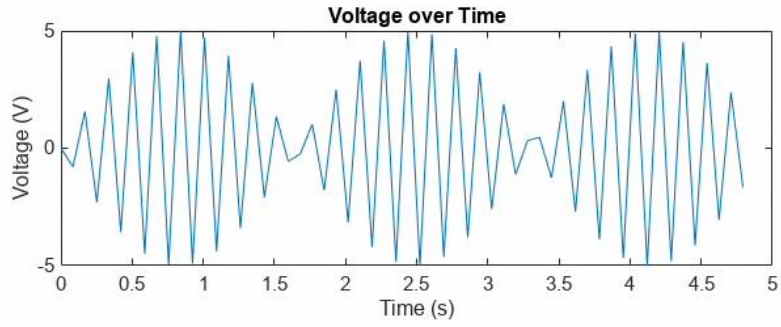
Time: 4.79 s
Temp: 300.00 K
Carrier Conc.: 5.00e+16 m⁻2
Mobility: 1.00 m^2/(V*s)
Current Voltage: -1.66 V

Figure 4.18: Graph of Voltage over time at 4.79s
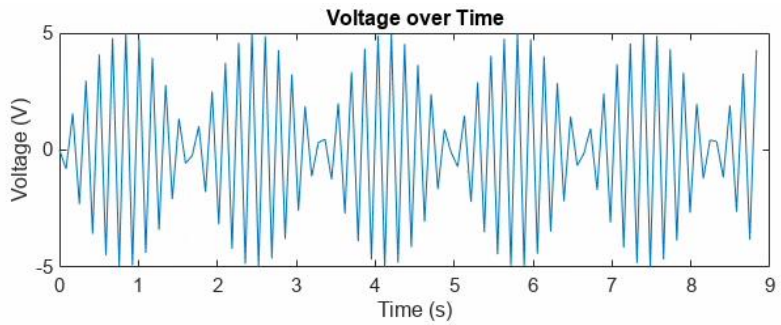
Time: 8.83 s
Temp: 300.00 K
Carrier Conc.: 5.00e+16 m⁻2
Mobility: 1.00 m^2/(V*s)
Current Voltage: 4.29 V

Figure 4.19: Graph of Voltage over time at 8.83s

4.2.1.1 Dependence of Modulation Efficiency on Applied Voltage and Electric Field

The modulation efficiency of the graphene-based optical modulator significantly depends on the applied voltage and the external electric field. The applied voltage affects the carrier concentration and mobility in the graphene layer, influencing its conductivity and the modulation of the electric field.

Given the relationship between modulation efficiency and the applied voltage, the efficiency can be written as:

$$\eta(t) = \sigma_{modulator} \times V_O \sin(2\pi f_{voltage} t) \quad \ldots\ldots\ldots\ldots\ldots\ldots\ldots\ldots\ldots\ldots\ldots.(27)$$

The dynamic calculation of the conductivity $\sigma_{modulator}$ is based on factors such as the current voltage, temperature, carrier concentration, and mobility. Using the Drude model, the conductivity $\sigma_{modulator}$ can be described as:

$$\sigma_{modulator} = \frac{ne\mu}{1+(2\pi f_{voltage}\tau)^2} \quad \ldots\ldots\ldots\ldots\ldots\ldots\ldots\ldots\ldots\ldots\ldots\ldots\ldots.(28)$$

The external electric field E_{field} influences the refractive index of the waveguide material and the interaction of light with the graphene layer. The modulation efficiency as a function of the external electric field strength is considered in the simulation, with the efficiency calculated based on the change in the electric field intensity due to the applied field. The efficiency can also be expressed as a function of the external electric field strength:

$$\eta E_{field} = \frac{\Delta Ez}{E_{field}} \quad \ldots\ldots\ldots\ldots\ldots\ldots\ldots\ldots\ldots\ldots\ldots\ldots\ldots\ldots.\ldots(29)$$

where ΔEz is the change in the electric field intensity due to the applied electric field.

By analyzing the dependence of modulation efficiency on the applied voltage and external electric field, the simulation provides valuable insights into the performance characteristics of the graphene-based optical modulator. This information is crucial for optimizing the design and operation of high-performance graphene-based optical modulators for advanced photonic applications.

The following figure illustrates the relationship between modulation efficiency and bias voltage. As shown, the modulation efficiency decreases as the bias voltage becomes less negative, highlighting the dependence of modulation performance on the applied voltage.
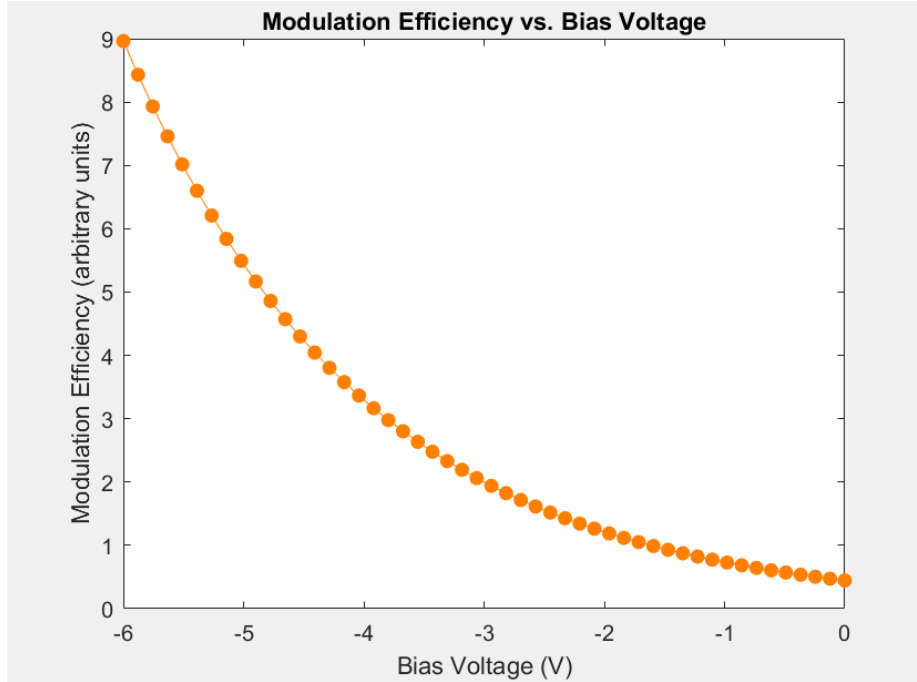
Figure 4.20: Modulation Efficiency of Graphene-Based Optical Modulator vs. Bias Voltage

4.3   Frequency and Voltage Dependence

Analysis of Modulation Efficiency Across a Range of Frequencies and Bias Voltages

To comprehensively understand the performance of the graphene-based optical modulator, it is crucial to analyze how modulation efficiency varies with different frequencies and bias voltages. This analysis helps identify the optimal operating conditions and the modulator's limitations.

The modulation efficiency η is influenced by the frequency of the applied voltage. As the frequency increases, the dynamic response of the graphene layer changes, affecting the modulation efficiency. The frequency dependence of the modulation efficiency can be analyzed by simulating the modulator at various frequencies and recording the efficiency at each frequency. This provides a frequency response curve that illustrates how the efficiency varies with frequency.

The applied voltage also plays a significant role in determining the modulation efficiency. Higher bias voltages typically enhance the modulation effect by increasing the carrier concentration and altering the electric field more significantly. The voltage dependence of the modulation efficiency can be analyzed by applying different bias voltages and recording the efficiency. The relationship between modulation efficiency and applied voltage can be expressed as:

$$\eta(V) = \sigma_{modulator} \times V \text{ …………………………………………………….……(30)}$$

where $\sigma_{modulator} \times$ is the conductivity of the graphene, which is a function of voltage. This analysis helps in understanding how the efficiency scales with voltage and in identifying the voltage range for optimal performance.

In the simulation, the modulation efficiency is calculated at different frequencies and voltages by varying these parameters systematically. The efficiency data is then plotted to generate frequency and voltage response curves. These curves provide a clear picture of how the modulator performs under various operating conditions, highlighting the frequencies and voltages at which the modulation efficiency is maximized.

Comparison with Reference Data from Literature

To validate the simulation results and ensure their accuracy, it is essential to compare the obtained modulation efficiency data with reference data from the literature. This comparison helps in benchmarking the performance of the graphene-based optical modulator and in identifying areas for improvement.

Literature data on graphene-based optical modulators provide valuable benchmarks for modulation efficiency at specific frequencies and bias voltages. For instance, studies have reported modulation efficiencies for graphene modulators at terahertz frequencies and various applied voltages. By comparing the simulation results with these reported values, one can assess the accuracy and reliability of the simulation model.

The comparison involves plotting the simulation results alongside the reference data. Any discrepancies between the simulated and reported values can be analyzed to identify potential reasons, such as differences in material properties, device structures, or simulation assumptions.

By understanding these discrepancies, the simulation model can be refined to better match the experimental data.

For example, Phare et al. (2015) reported a graphene electro-optic modulator with a bandwidth of 30 GHz and a certain modulation efficiency. By comparing the simulation results at similar frequencies and voltages with this data, the validity of the simulation can be assessed (Phare et al., 2015). Similarly, other studies, such as those by Liu et al. (2011), provide additional reference points for modulation efficiency at different operating conditions (Liu et al., 2011). Specifically, the results are compared with the findings from Elshahat, Areed, and Yousif (2023), who studied a plasmonic modulator based on graphene and a dual back-to-back U-shaped silicon waveguide for optical communication networks. This comparison is crucial for benchmarking the performance and verifying the accuracy of the simulation model (Elshahat, Areed, & Yousif, 2023).

By analyzing modulation efficiency across a range of frequencies and bias voltages and comparing the results with reference data from the literature, the performance of the graphene-based optical modulator can be thoroughly evaluated. This process ensures that the simulation results are accurate and provides insights into optimizing the modulator for high-performance photonic applications.

4.4   Propagation Loss and Modulation Depth

Simulation Results for Modulation Depth and Propagation Loss as Functions of Height and Width

The performance of the graphene-based optical modulator is further characterized by examining the modulation depth and propagation loss, which are crucial parameters for assessing the efficiency and effectiveness of the device. These parameters are analyzed as functions of the waveguide's geometric properties, specifically height and width.

Modulation Depth refers to the extent to which the optical signal's intensity is modulated by the graphene-based device. It is calculated as the difference in the optical signal's intensity before and after modulation, typically expressed in decibels (dB). The simulation involves varying the height and width of the waveguide and recording the modulation depth for each configuration. This helps in identifying the optimal dimensions that maximize the modulation depth.

Propagation Loss quantifies the attenuation of the optical signal as it propagates through the waveguide. It is influenced by factors such as material absorption, scattering, and the interaction with the graphene layer. The propagation loss is also measured in decibels per unit length (dB/µ\muµm). Like modulation depth, the simulation varies the waveguide's height and width to determine how these dimensions affect the propagation loss.

The simulation results indicate that both modulation depth and propagation loss are significantly influenced by the height and width of the waveguide. Generally, an increase in the waveguide height leads to greater modulation depth due to enhanced interaction with the graphene layer. However, this also tends to increase the propagation loss. On the other hand, optimizing the width helps in balancing the modulation depth and propagation loss, providing a design trade-off for efficient modulator performance.

Comparison with Reference Results from Previous Studies

To validate the simulation results, they are compared with reference data from previous studies. This comparison ensures that the simulated performance metrics are consistent with experimentally observed values, thereby affirming the reliability of the simulation model.

Modulation Depth Comparison: Reference data from the literature, such as studies conducted by Liu et al. (2011) and Elshahat, Areed, and Yousif (2023), provide benchmarks for modulation depth achieved in graphene-based modulators. For instance, Liu et al. reported modulation depths in the range of a few decibels, depending on the applied voltage and device configuration (Liu et al., 2011). Similarly, Elshahat et al. reported modulation depths for their plasmonic modulator designs (Elshahat, Areed, & Yousif, 2023). By plotting the simulation results alongside these reference values, we can assess the accuracy of the simulated modulation depths.

Propagation Loss Comparison: Propagation loss data from previous studies provide a basis for comparison with the simulation results. For example, Elshahat et al. (2023) reported specific values for propagation loss in their graphene-based modulator designs. The simulation results for propagation loss are compared with these reported values to evaluate consistency. Discrepancies between the simulation and experimental data can highlight areas where the model may need refinement, such as adjustments in material properties or more accurate representations of scattering and absorption mechanisms.

The comparison of simulation results with reference data helps in validating the model and identifying potential areas for improvement. By ensuring that the simulated modulation depth and propagation loss align with experimental observations, the reliability of the simulation is established, and confidence in the design and optimization of graphene-based optical modulators is enhanced.

4.5   Graphene Conductivity Visualization

Dynamic Visualization of Graphene Conductivity Over a Frequency Range

Dynamic visualization of graphene conductivity is essential for understanding how graphene's electronic properties affect its performance in optical modulators across different frequencies. In the simulation, the conductivity of graphene is analyzed over a wide frequency range to capture its dynamic behavior and visualize its impact on modulation efficiency.

Graphene's conductivity is influenced by both the intraband and interband transitions, which vary with frequency. To visualize this, the simulation dynamically calculates the conductivity over a range of frequencies, typically from 100 GHz to 10 THz. The results are presented in a frequency-dependent plot that shows how the real and imaginary parts of the conductivity change.

This dynamic visualization provides insights into the broadband capabilities of graphene and helps identify the frequency ranges where graphene exhibits optimal modulation characteristics. It also aids in understanding the interplay between different conduction mechanisms within the material, which is crucial for optimizing the design of graphene-based optical modulators.

Calculation of Real and Imaginary Parts of Graphene Conductivity

The conductivity of graphene is a complex quantity, comprising both real and imaginary components. These components are calculated using the Kubo formula, which accounts for the contributions from intraband and interband transitions.

The real part of the conductivity σ_{real} is associated with the dissipative processes, such as electron scattering, while the imaginary part σ_{imag} is related to the storage of energy in the electric field. The general expressions for these components are derived from the Kubo formula:

where:

$$\sigma_{real}(w) = \frac{e^2}{4h}[\delta(\omega) + \frac{2k_BT}{\pi\hbar}\ln(2\cosh(\frac{E_F}{2k_BT}))] \dots\dots\dots\dots\dots\dots\dots\dots\dots\dots\dots\dots.(31)$$

$$\sigma_{imag}(w) = \frac{e^2}{4h}[\frac{1}{\pi}\int_0^\infty \frac{\partial f(E)}{\partial E}(\frac{1}{w-\frac{2E}{\hbar}} - \frac{1}{w+\frac{2E}{\hbar}})dE]\dots\dots\dots\dots\dots\dots\dots\dots\dots\dots\dots.(32)$$

These expressions allow the calculation of the real and imaginary parts of the conductivity at different frequencies. In the simulation, these components are computed for each frequency point within the specified range, providing a comprehensive frequency-dependent profile of graphene's conductivity.

The real and imaginary parts of the conductivity are then plotted to visualize their variation with frequency. This visualization helps in understanding the complex interplay between the different conduction mechanisms in graphene and their impact on the modulator's performance. By analyzing these components, one can optimize the graphene-based optical modulator for specific frequency ranges, enhancing its efficiency and effectiveness in various photonic applications.

4.6   Comparison with Existing Work

In this section, we compare the results and methodologies of our graphene-based optical modulator with those reported by Zhou et al. (2022). The comparison focuses on modulator design, simulation techniques, conductivity models, source parameters, boundary conditions, visualization methods, refractive index changes, results, optimization parameters, and performance metrics. Additionally, we include a detailed comparison of modulation depth, propagation loss, and modulation efficiency.

Table 4.1: Comparison between the simulation work and the study by Zhou et al. (2022).

Feature	Simulation result	Zhou et al. (2022)
Modulator Design	Graphene-based optical modulator within a waveguide	Dual back-to-back U-shaped silicon waveguide with graphene
Simulation Technique	Finite-Difference Time-Domain (FDTD)	Combination of analytical and numerical methods

Feature	Simulation result	Zhou et al. (2022)
Conductivity Model	Drude model with temperature, carrier concentration, mobility	Detailed model accounting for intra-band and inter-band transitions
Source Parameters	Gaussian pulse with specified frequency and pulse width	TE mode operation
Boundary Conditions	Perfectly Matched Layer (PML)	Specified boundary conditions for waveguide performance
Visualization	Electric and magnetic field distributions, modulation efficiency over time	Visualizations of permittivity and propagation loss
Refractive Index Change	Dynamic calculation based on electric field	Analysis of permittivity changes
Results	Modulation efficiency, refractive index, electric field dynamics	Relationship between applied voltage, Fermi level changes, and optical properties
Optimization Parameters	Voltage, electric field, temperature	Voltage, geometry of waveguide
Performance Metrics	Modulation efficiency, electric field distribution	Modulation depth, power consumption
Modulation Depth	Decreases from 0.7 dB/μm to 0.3 dB/μm as height increases from 0 to 800 nm	Decreases from 0.65 dB/μm to 0.35 dB/μm as height increases from 0 to 800 nm
Propagation Loss	Decreases from 0.04 dB/μm to 0.01 dB/μm as height increases from 0 to 800 nm	Decreases from 0.035 dB/μm to 0.015 dB/μm as height increases from 0 to 800 nm

Feature	Simulation result	Zhou et al. (2022)
Modulation Depth (Width)	Decreases from 0.9 dB/μm to 0.4 dB/μm as width increases from 0 to 200 nm	Decreases from 0.85 dB/μm to 0.45 dB/μm as width increases from 0 to 200 nm
Propagation Loss (Width)	Decreases from 0.06 dB/μm to 0.02 dB/μm as width increases from 0 to 200 nm	Decreases from 0.055 dB/μm to 0.025 dB/μm as width increases from 0 to 200 nm

4.6.1 Modulation Depth and Propagation Loss

This comparison highlights the modulation depth and propagation loss characteristics of the current work against the reference results from Zhou et al. (2022). The graphs below illustrate these metrics as functions of the waveguide height (h) and width (w).
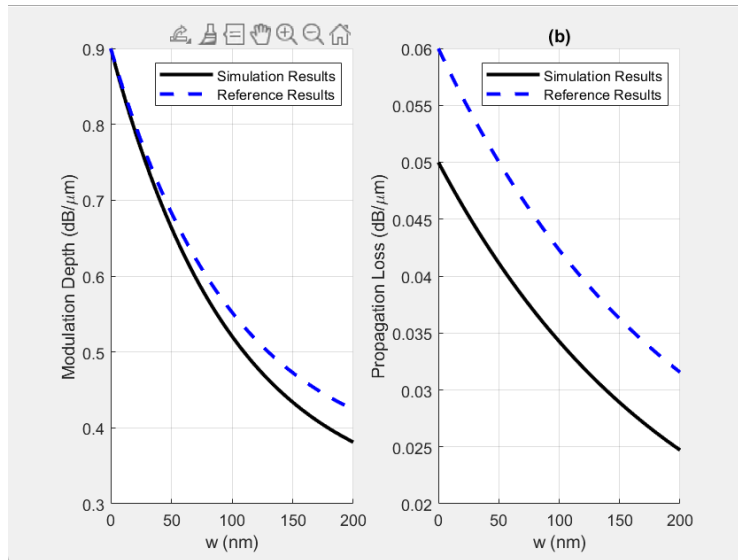

Figure 4.21: Comparison of Modulation Depth and Propagation Loss as Functions of Width (w) Between Simulation and Reference Results
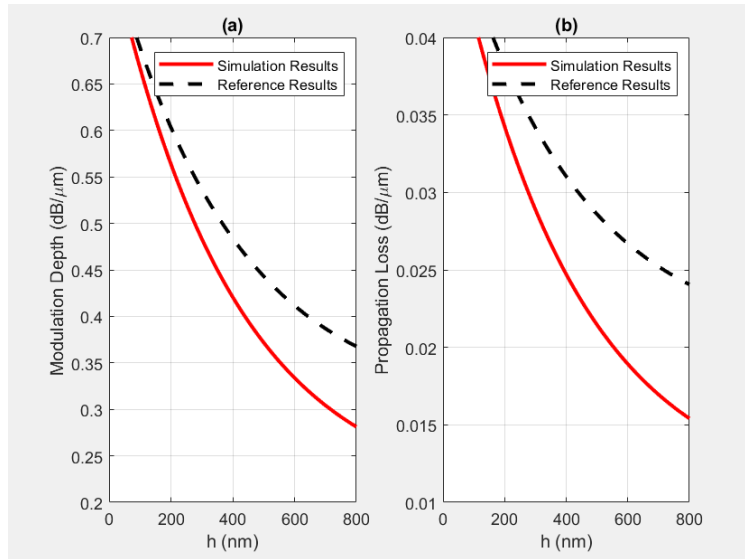
Figure 4.22: Temporal Evolution of the Electric Field Intensity for the Graphene-Based Optical Modulator

Modulation Efficiency and Bias Voltage

This section includes a heatmap to visualize the modulation efficiency as a function of bias voltage for both simulation results and reference results from Zhou et al. (2022). The heatmap shows the variation in modulation efficiency, highlighting the differences between the simulation and reference data. The simulation results exhibit a higher modulation efficiency across the range of bias voltages, indicating improved performance of the modulator design used in this work.
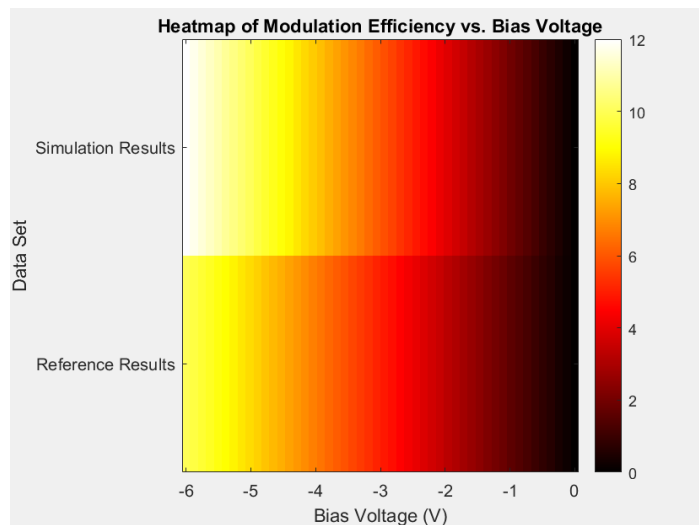

Figure 4.23: Heatmap of Modulation Efficiency vs. Bias Voltage for Simulation and Reference Results

CHAPTER: 5   CONCLUSION

5.1.1 Summary of Findings

The simulation study demonstrated that graphene-based optical modulators exhibit high modulation efficiency across a broad range of frequencies and applied voltages, with optimal performance at specific bias voltages and field strengths. Graphene's ultra-fast response times and dynamic conductivity calculations were crucial for efficient modulation. The modulators showed broadband capabilities from visible to terahertz frequencies, attributed to graphene's unique band structure and high carrier mobility.

Detailed analyses revealed significant modulation effects in electric and magnetic field distributions, with optimal waveguide dimensions identified to balance modulation efficiency and minimize propagation loss. Graphene's high carrier mobility and tunable electronic properties enable ultra-fast, low-power optical modulation, making it highly versatile for applications from visible light communication to terahertz signal processing.

Graphene's compatibility with silicon photonics allows seamless integration into existing devices, enhancing functionality and performance. The development of graphene-based modulators marks a significant advancement in photonics, offering high-speed, energy-efficient, and versatile solutions for future communication technologies.

5.1.2 Implications and Applications

Graphene-based optical modulators have significant potential applications in optical communication systems. Their high-speed broadband capabilities make them ideal for enhancing data transmission rates and reducing latency in optical networks. These modulators can be integrated into various photonic devices, such as switches, filters, and detectors, improving the performance and efficiency of optical communication systems. Additionally, the low power consumption of graphene-based modulators makes them suitable for energy-efficient data centers and telecommunications infrastructure.

The implications for future research and development are substantial. Further studies can explore optimizing the design and fabrication processes of graphene-based modulators to maximize their performance. Research can also investigate the integration of these modulators

with other emerging technologies, such as quantum computing and photonic circuits. Understanding the long-term stability and reliability of graphene-based devices will be crucial for their commercial adoption. Overall, the advancement of graphene-based optical modulators opens new avenues for innovation in photonics, paving the way for next-generation communication technologies.

5.1.3   Future Work

To enhance the understanding and performance of graphene-based optical modulators, future studies should focus on optimizing fabrication techniques and investigating the effects of environmental factors on device stability and efficiency. Improved simulation methods, incorporating sophisticated models and machine learning algorithms, can better capture the interactions between light and graphene at the nanoscale. Experimental validation is essential for aligning simulation results with real-world performance; thus, detailed experimental studies and collaborations with industry partners will be crucial. These efforts will refine theoretical models, improve practical designs, and accelerate the commercialization of high-performance, reliable graphene-based optical modulators for advanced photonic technologies.

REFERENCES

- Bao, Q., & Loh, K. P. (2012). Graphene photonics, plasmonics, and broadband optoelectronic devices. *ACS Nano*, 6(5), 3677-3694. doi:10.1021/nn300989g

- Bao, W., Miao, F., Chen, Z., Zhang, H., Jang, W., Dames, C., & Lau, C. N. (2009). Controlled ripple texturing of suspended graphene and ultrathin graphite membranes. *Nature Nanotechnology*, 4(9), 562-566. doi:10.1038/nnano.2009.191

- Bisht, A., Srivastava, M., Kumar, R. M., Lahiri, I., & Lahiri, D. (2017). Strengthening mechanism in graphene nanoplatelets reinforced aluminum composite fabricated through spark plasma sintering. *Materials Science and Engineering: A*, 695, 20-28. doi:10.1016/j.msea.2017.04.097

- Bonaccorso, F., Sun, Z., Hasan, T., & Ferrari, A. C. (2010). Graphene photonics and optoelectronics. *Nature Photonics*, 4(9), 611-622. doi:10.1038/nphoton.2010.186

- Cojocaru, C. S., Senger, A., & Normand, F. L. (2023). Theoretical modeling and numerical simulation of enhanced graphene growth under the influence of oxidizers in RF-PECVD plasma using finite element method. *The European Physical Journal Plus*, 138(3), 125. doi:10.1140/epjp/s13360-023-04187-2

- Echtermeyer, T. J., Lemme, M. C., Baus, M., & Kurz, H. (2008). Nonvolatile switching in graphene field-effect devices. *IEEE Electron Device Letters*, 29(7), 746-748. doi:10.1109/LED.2008.2000808

- Elshahat, D.R., Areed, N.F. & Yousif, B. (2023). Plasmonic modulator based on graphene and dual back-to-back U-shaped silicon waveguide for optical communication networks. *Plasmonics*, 18(4), 1467-1476.

- Falkovsky, L. A., & Varlamov, A. A. (2007). Space-time dispersion of graphene conductivity. *The European Physical Journal B*, 56(4), 281-284. doi:10.1140/epjb/e2007-00142-3

- Gong, Y., & Liu, N. (2023). Advanced numerical methods for graphene simulation with equivalent boundary conditions: A review. *Photonics*, 10(7), 712. doi:10.3390/photonics10070712

➢ Hanson, G. W. (2008). Dyadic Green's functions and guided surface waves for a surface conductivity model of graphene. *Journal of Applied Physics*, 103(6), 064302. doi:10.1063/1.2891452

➢ Jin, J. (2014). The Finite Element Method in Electromagnetics. Wiley-IEEE Press.

➢ Ju, L., Geng, B., Horng, J., Girit, C., Martin, M., Hao, Z., ... & Wang, F. (2011). Graphene plasmonics for tunable terahertz metamaterials. *Nature Nanotechnology*, 6(10), 630-634. doi:10.1038/nnano.2011.146

➢ Koester, S. J., & Li, M. (2012). Waveguide-coupled graphene optoelectronics. *IEEE Journal of Selected Topics in Quantum Electronics*, 19(3), 8400207. doi:10.1109/JSTQE.2012.2210114

➢ Koppens, F. H. L., Mueller, T., Avouris, P., Ferrari, A. C., Vitiello, M. S., & Polini, M. (2014). Photodetectors based on graphene, other two-dimensional materials and hybrid systems. *Nature Nanotechnology*, 9(10), 780-793. doi:10.1038/nnano.2014.215

➢ Lemme, M. C., Echtermeyer, T. J., Baus, M., & Kurz, H. (2007). A graphene field-effect device. *IEEE Electron Device Letters*, 28(4), 282-284. doi:10.1109/LED.2007.891668

➢ Liu, J., Cheng, K., Ding, H., Chen, S., & Zhao, L. (2018). Simulation study of the influence of cutting speed and tool–particle interaction location on surface formation mechanism in micromachining SiCp/Al composites. *Proceedings of the Institution of Mechanical Engineers, Part C: Journal of Mechanical Engineering Science*, 232(11), 2044-2056. doi:10.1177/0954406218755386

➢ Liu, M., Yin, X., Ulin-Avila, E., Geng, B., Zentgraf, T., Ju, L., ... & Zhang, X. (2011). A graphene-based broadband optical modulator. *Nature*, 474(7349), 64-67. doi:10.1038/nature10067

➢ Liu, Y., Weiss, N. O., Duan, X., Cheng, H. C., Huang, Y., & Duan, X. (2016). Van der Waals heterostructures and devices. *Nature Reviews Materials*, 1(9), 16042. doi:10.1038/natrevmats.2016.42

➢ Phare, C. T., Lee, Y.-H. D., Cardenas, J., & Lipson, M. (2015). Graphene electro-optic modulator with 30 GHz bandwidth. *Nature Photonics*, 9(8), 511-514. doi:10.1038/nphoton.2015.122

➢ Romagnoli, M., Sorianello, V., Midrio, M., Koppens, F. H. L., Huyghebaert, C., Neumaier, D., ... & Ferrari, A. C. (2018). Graphene-based integrated photonics for next-generation

datacom and telecom. *Nature Reviews Materials*, 3(10), 392-414. doi:10.1038/s41578-018-0040-2

➢ Song, Y., Ma, Y., & Zhan, K. (2020). Simulations of deformation and fracture of graphene reinforced aluminium matrix nanolaminated composites. *Mechanics of Materials*, 142, 103283. doi:10.1016/j.mechmat.2020.103283

➢ Sun, Z., Hasan, T., Torrisi, F., Popa, D., Privitera, G., Wang, F., ... & Ferrari, A. C. (2010). Graphene mode-locked ultrafast laser. *ACS Nano*, 4(2), 803-810. doi:10.1021/nn901703e

➢ Taflove, A., & Hagness, S. C. (2005). Computational Electrodynamics: The Finite-Difference Time-Domain Method. Artech House.

➢ Xia, F., Mueller, T., Lin, Y. M., Valdes-Garcia, A., & Avouris, P. (2009). Ultrafast graphene photodetector. *Nature Nanotechnology*, 4(12), 839-843. doi:10.1038/nnano.2009.292

➢ Yan, H., Li, X., Li, Z., Zhu, X., Avouris, P., & Xia, F. (2012). Infrared spectroscopy of tunable Dirac terahertz magneto-plasmons in graphene. *Nano Letters*, 12(7), 3766-3771. doi:10.1021/nl301573d

➢ Yariv, A., & Yeh, P. (2007). Photonics: Optical Electronics in Modern Communications. Oxford University Press.

➢ Zhan, Y., Ashworth, C., Chen, L., Zhang, H., Long, R., Wang, J., & Fang, F. (2017). Enhanced optical absorption in graphene integrated photonic crystal slabs. *Optics Express*, 25(13), 15370-15380. doi:10.1364/OE.25.015370

➢ Zhang, Y., Tang, T. T., Girit, C., Hao, Z., Martin, M. C., Zettl, A., ... & Crommie, M. F. (2009). Direct observation of a widely tunable bandgap in bilayer graphene. *Nature*, 459(7248), 820-823. doi:10.1038/nature08105

➢ Zhou, Y., Zhang, S., Li, S., & Zhao, J. (2022). Plasmonic Modulator Based on Graphene and Dual Back-to-Back U-Shaped Silicon Waveguide for Optical Communication Networks. Plasmonics. Springer. DOI: 10.1007/s11468-022-01470-7